A Comparison of Spray-drying and Co-precipitation for the Generation of Amorphous Solid Dispersions (ASDs) of Hydrochlorothiazide and Simvastatin

Monika Myślińska , Michael W. Stocker , Steven Ferguson , Anne Marie Healy

PII: S0022-3549(23)00064-3
DOI: https://doi.org/10.1016/j.xphs.2023.02.012
Reference: XPHS 3019

To appear in: *Journal of Pharmaceutical Sciences*

Received date: 15 November 2022
Revised date: 13 February 2023
Accepted date: 13 February 2023

Please cite this article as: Monika Myślińska , Michael W. Stocker , Steven Ferguson , Anne Marie Healy , A Comparison of Spray-drying and Co-precipitation for the Generation of Amorphous Solid Dispersions (ASDs) of Hydrochlorothiazide and Simvastatin, *Journal of Pharmaceutical Sciences* (2023), doi: https://doi.org/10.1016/j.xphs.2023.02.012

A Comparison of Spray-drying and Co-precipitation for the Generation of Amorphous Solid Dispersions (ASDs) of Hydrochlorothiazide and Simvastatin

Monika Myślińska[1,3,4], Michael W. Stocker[2, 3], Steven Ferguson[2,3,4,5,6], Anne Marie Healy*[1,3,4]

1. School of Pharmacy and Pharmaceutical Sciences, Panoz Institute, Trinity College Dublin, Dublin 2, Ireland
2. School of Chemical and Bioprocess Engineering, University College Dublin, Dublin 4, Ireland
3. SSPC, The Science Foundation Ireland Research Centre for Pharmaceuticals
4. EPSRC-SFI Centre for Doctoral Training in Transformative Pharmaceutical Technologies, Ireland
5. I-Form, The SFI Research Centre for Advanced Manufacturing, School of Chemical and Bioprocess Engineering, University College Dublin, Dublin 4, Ireland
6. National Institute for Bioprocess Research and Training, Dublin, Ireland

*Corresponding author information:

Email address: healyam@tcd.ie

Address: School of Pharmacy and Pharmaceutical Sciences

Trinity College Dublin

The University of Dublin

Dublin 2, Ireland

Phone number: +353 1 896 2809

Abstract

Co-processing of APIs, the practice of creating multi-component APIs directly in chemical processing facilities used to make drug substance, is gaining increased attention with a view to streamlining manufacturing, improving supply chain robustness and accessing enhanced product attributes in terms of stability and bioavailability. Direct co-precipitation of amorphous solid dispersions (ASDs) at the final step of chemical processing is one such example of co-processing. The purpose of this work was to investigate the application of different advanced solvent-based processing techniques - direct co-precipitation (CP) and the benchmark well-established spray-drying (SD) process - to the production of ASDs comprised of a drug with a high T_g (hydrochlorothiazide, HCTZ) or a low T_g (simvastatin, SIM) molecularly dispersed in a PVP/VA 64 or Soluplus® matrix. ASDs of the same composition were manufactured by the two different methods and were characterised using powder X-ray diffraction (PXRD), modulated differential scanning calorimetry (mDSC), attenuated total reflectance Fourier transform infrared spectroscopy (ATR-FTIR) and scanning electron microscopy (SEM). Both methods produced ASDs that were PXRD amorphous, with some differences, depending on the process used, in glass transition temperature and particle size distribution. Irrespective of

manufacturing method used, all ASDs remained PXRD amorphous when subjected to high relative humidity conditions (75% RH, 25°C) for four weeks, although changes in the colour and physical characteristics were observed on storage for spray-dried systems with SIM and PVP/VA 64 copolymer. The particle morphology differed for co-precipitated compared to spray dried systems, with powder generated by the former process being comprised of more irregularly shaped particles of larger particle size when compared to the equivalent spray-dried systems which may enable more streamlined drug product processes to be used for CP materials. These differences may have implications in downstream drug product processing. A limitation identified when applying the solvent/anti-solvent co-precipitation method to SIM was the high antisolvent to solvent ratios required to effect the precipitation process. Thus, while similar outcomes may arise for both co-precipitation and spray drying processes in terms of ASD critical quality attributes, practical implications of applying the co-precipitation method and downstream processability of the resulting ASDs should be considered when choosing one solvent-based ASD production process over another.

Keywords: Amorphous Solid Dispersion(s) (ASD); Formulation; Physicochemical properties; Co-precipitation; Co-processed APIs; Spray drying

Introduction

Co-processing active pharmaceutical ingredients (APIs) with inert excipients has recently gained attention as a strategy for improving the critical quality attributes (CQAs), product stability and manufacturing processes of composite API-excipient materials and consequently improving drug product efficacy and supply chains.[1,2] Co-processing achieves this by creating multicomponent systems of APIs and non-active substances that exploit the properties of the non-active component to stabilise a desirable solid form and/or improve the processability of the API powder. Notably, the non-active components are introduced to the API during drug substance (DS) manufacturing, typically at the point of API isolation. This means that the co-processed API can be produced in a drug substance facility without requiring additional unit operations or isolation steps.[1] Co-processed APIs can also address the increasingly prevalent problem of low aqueous solubility of new chemical entities (NCEs) that restrict the performance of NCEs formulated as oral solid dosage forms (OSDs).[3-4] Low aqueous solubility can be associated with suboptimal dose uptake[5] and increased gastrointestinal mucosal toxicity.[6] Numerous strategies have been developed to resolve this issue by chemical or physical modifications of the compound and include particle micronisation,[7] complexation,[8] salt formation,[9,10] cocrystallization,[11] ionic liquid formation[12-14] or amorphous solid dispersions (ASDs).

ASDs exploit the favourable properties of the amorphous form of the API that arise due to the lack of a crystalline lattice, and the lower energy barrier this presents in order for the solid form to be disrupted, leading to an increase in the API aqueous solubility.[15,16] Combining the amorphous form of the pure drug with a polymer to form a molecularly dispersed solid solution can mitigate the stability problems

associated with amorphous API forms. The polymer functions as a crystallization inhibitor during storage of the formulation or during drug dissolution to maintain a supersaturated solution and prevent the metastable amorphous form from crystallizing into a more stable (and less soluble) form.[17] However, there are still some drawbacks associated with this technology that require further investigation regarding the uncontrolled recrystallization of the amorphous form in the solid form during storage, dissolution or in downstream processing operations. The factors affecting this crystallization are known to include the individual properties of the API molecule, the type of the manufacturing method employed for forming the ASD and storage conditions.[17-19] There are a number of processes that are used to generate ASDs and these can be divided into thermal, milling, solvent and lyophilization based methods.[20] The chosen manufacturing method is often dependent on the characteristics of the API molecule. Compounds that are not soluble in volatile solvents are often subjected to fusion-based methods such as hot melt extrusion (HME) or, more recently, acoustic fusion.[21] APIs that have high melting points but are soluble in organic or aqueous solvents may be processed by solvent-based methods such as spray drying, electrospraying[22] or co-precipitation.[20]

This work serves to investigate the differences in the properties of ASDs produced by spray drying and co-precipitation for two APIs with different physicochemical properties and ascertain the benefits, if any, of employing one technique over the other. One of the advantages of both spray drying and co-precipitation is that they can be performed below the melting temperature of the API, which is particularly beneficial when working with thermally labile compounds.[20] This is an advantage over melt-based methods, such as HME, in which the processing temperatures can affect either chemical degradation of the APIs or their lack of complete transformation into the amorphous state.[23] Moreover, further mechanical processing after the HME process, involving milling or pelletization, might also affect the solid state form of the drug. While spray drying is well established and commonly used to manufacture ASDs commercially, it usually requires large solvent volumes and specialized equipment which increases the cost and complexity of the process.[1,24] In contrast, co-precipitation is of interest as it can be carried out using common equipment which is readily available in DS manufacturing facilities (such as high shear wet mills) that can be unobtrusively incorporated into existing process streams.[24] The solvents used in solvent-based processes should belong to Class 2 or Class 3 as specified in the International Council on Harmonization guideline Q3C (R6)[25] on the acceptable amounts of residual solvents in pharmaceuticals. Subsequent to the co-precipitation process powders can be isolated from the suspension and solvent removed by filtration and/or evaporation unit operations. If filtered, the solvents in the mother liquor can be discarded following current protocols on waste management or recovered, if possible, using current technologies.[26]

The successful development of the co-precipitation process is largely related to the solubility of both the amorphous or crystalline forms at a given temperature in the solvent/antisolvent system used.[27-30] In contrast to crystallization processes where a slow precipitation rate is desirable to control the nucleation and crystal growth, a fast precipitation rate is required to obtain an amorphous coprecipitated form.[30] Since all formulation components should be almost insoluble in one of the solvents, the supersaturation induced by interaction of two miscible solvents triggers the precipitation.

Process and feed parameters applied in the technique affect the thermodynamic and kinetic events leading to co-precipitation of ASDs. Frank et al. reported that co-precipitated systems obtained without mixing were partially crystalline when analysed by PXRD, whereas for equivalent systems prepared using a low shear rate by means of a magnetic stirrer bar or overhead stirrer, some residual crystallinity was found by DSC. The same systems prepared using a homogenizer produced fully amorphous powders.[31] Mixing devices provide different shearing forces, impacting the homogenous distribution of the supersaturated state of formulation components in the system and interactions of the API-polymer-solvent mixture that can influence the uniformity of the generated precipitated suspension. However, as other studies have found no evidence of crystallinity when using overhead mixing[32], the homogeneity of the system is not solely dependent on the mixer type but also depends on the individual properties of formulation components, drug loading and the geometry of the equipment used.

APIs with both low and high melting points can be processed by this method and, in contrast to spray drying, it has also been used to successfully process APIs with low solubility in volatile solvents.[24] Based on recent reports, co-precipitation may increase the possible drug load of the material and increase the density of the powders[33] which is advantageous in downstream processing as it improves flowability and compressibility of the powder.[34] This technology is believed to be a platform compatible with both batch and continuous manufacturing.[35,15] Moreover, it has been suggested that the API and polymer co-precipitate may be defined as a drug substance[1] from a regulatory perspective, as opposed to spray dried or hot melt extruded systems which have typically been classified as drug product intermediates.[1,24] This change in the classification system, that has already been implemented in the case of cocrystal formulations, may optimize the time and energy constraints spent on the final drug product on the manufacturing site.[36,37,15]

The different kinetic and thermal events involved in the different pharmaceutical processes are likely to produce ASDs with different intermolecular compositions,[38] and thus possibly different physical stabilities. While different manufacturing processes can yield powders with the same drug:polymer ratios, they also may affect the components' interactions at the molecular level, resulting in homogenously mixed components, phase separated systems or systems that are homogenously mixed but with some residual crystallinity.[39] In the co-precipitation technique, differences in components' individual solubilities in the final solvent mixture may result in powders with a much increased or decreased drug:polymer ratio when compared to their theoretical ratios. Therefore, if co-precipitation methods are to be employed in commercial production of ASD API forms, a broader literature and understanding of differences in the critical quality attributes of co-precipitate ASDs compared to those prepared by more established techniques is required, as is information on which, if any, of the polymers used in the formulation is superior in terms of amorphous form stabilization.

There have been a limited number of previous reports where comparisons of different methods for producing ASDs of the same API have been made, and few reports where a direct comparison of spray drying and co-precipitation techniques has been undertaken.[31-32,40] Caron *et al*. demonstrated that for sulfadimidine and sulfathiazole co-processed with PVP, the composition range over which

homogeneous glassy solution ASDs could be generated was much broader for spray drying than milling, although the glass transition temperature (T_g) of the generated ASDs for a particular API/PVP ratio did not depend on the processing technique used.[38] However, there are other reports in the literature where neither the amorphous character nor stability of the API was altered by employing one technique over the other.[41,42] Most studies of co-precipitation of ASDs have involved the API dispersed in an ionic polymer with an aqueous medium being used as the antisolvent.[43-45] In recent years there have been more reports on the liquid antisolvent co-precipitation technique with the use of non-ionic polymers and organic solvents.[32,40] Further comparative work examining the quality and stability of the products produced by these methods would allow the applicability of each process to be mapped out and methodically inform which process is most suitable for which API.

In this work spray drying and co-precipitation were investigated with respect to the final critical quality attributes of the produced powders to establish if there are any differences in product characteristics that can be attributed to the processing technique and to establish whether either of these techniques is superior to the other in terms of ASD stability. Moreover, we compared ASD systems containing structurally different APIs to assess whether the different physical characteristics would impact the choice of manufacturing method. The results presented in this article aim to inform the selection of aforementioned two solvent-based manufacturing processes for forming ASDs.

Materials and Methods

Materials

Hydrochlorothiazide (HCTZ) and simvastatin (SIM) were purchased from Glentham Life Sciences Ltd. (Corsham, UK). Polymers, polyvinyl pyrrolidine/vinyl acetate 60/40 (Kollidon VA64®, PVP/VA) and polyvinyl caprolactam–polyvinyl acetate–polyethylene glycol graft copolymer (Soluplus®) were obtained from BASF (Cork, Ireland). Ethanol (EtOH) was obtained from Corcoran Chemicals (Dublin, Ireland). Liquid nitrogen was purchased from BOC (Dublin, Ireland) while sodium chloride was obtained from Sigma Aldrich (Arklow, Ireland). Dichloromethane (DCM) and hexane were obtained from Sigma-Aldrich (Dorset, UK), deionised water (14.0 MΩ·cm) was obtained using an Elix 3 connected to a Synergy UV system (Millipore, UK).

Powder Production by Spray Drying (SD)

Drug and polymer were dissolved in a solvent composed of 95% (v/v) ethanol and 5% (v/v) deionised water. Solids were dissolved in ratios of 30:70 (w/w) and 40:60 (w/w) (drug:polymer) with total solute content of 2.5% (w/v) for HCTZ systems, and 5.0% (w/v) for SIM systems based on their respective solubilities in the solvent. The solutions were spray dried using a Büchi B-290 Mini spray dryer (BÜCHI Labortechnik AG, Flawil, Switzerland) equipped with a high efficiency cyclone. The spray dryer was equipped with a two-fluid nozzle with 0.7 mm nozzle tip and a 1.5 mm cap and nitrogen as the

atomizing gas. The parameters of the process were as follows: 78°C inlet temperature, 667 L/hr atomising nitrogen flow rate at standard temperature and pressure, 35 m^3/hr drying air flow rate and 6 mL/min solution feed rate. These parameters gave an outlet temperature between 40 to 44 °C.

Powder Production by Co-precipitation (CP)

The co-precipitation in this work was carried out in a 100 mL glass EasyMax™ reactor (Mettler Toledo, Greifense, Switzerland) agitated with an overhead stirrer with an upward pumping 38 mm diameter steel pitch blade impeller with 45° inclined blades (Figure S1).[46] The temperature in the vessel was controlled and monitored using iControl 5.5 (Mettler Toledo Software). The obtained co-precipitates of both APIs were isolated by filtration using sintered glass filters (Fisher Scientific, Dublin, Ireland) with a pore size of 10 – 20 µm. The filtration time varied in the range 2 – 4 minutes. The filtered solid was dried in a vacuum oven (Gallenkamp, Cambridge, United Kingdom) at 900 mbar, at 70°C for HCTZ samples and 40°C for SIM systems for 12 h, ground gently in a mortar with pestle, and left for a further 24 h in the vacuum oven. The process conditions used for the two APIs are detailed below.

HCTZ Systems

Drug and polymer were precipitated from solution using a solvent (ethanol) to antisolvent (hexane) ratio of 1:4 (v/v). Drug and polymer were dissolved in ethanol with total solid content of 5% (w/v) at 74°C on a hot plate (Stuart SD 162, Staffordshire, UK) using a magnetic stirrer at a rate of 400 rpm. Two drug:polymer ratios were used; 30:70 (w/w) and 40:60 (w/w). The solution, at approximately 40°C, was added to the antisolvent held at 10 °C at a rate of 5 mL/min with a syringe with a continuous overhead stirring at 600 rpm.

SIM Systems

Drug and polymer were precipitated from solution using a solvent (DCM) to antisolvent (hexane) ratio of 1:30 (v/v). Drug and polymer were dissolved in DCM with total solid content of 35% (w/v) at the drug:polymer ratios of 30:70 (w/w) and 40:60 (w/w). The feed solution was placed in an ice bath to cool it to approximately 2 °C before being added to the antisolvent held at -10 °C at a rate of 5 mL/min with a syringe with a continuous overhead stirring at 600 rpm.

Equilibrium Solubility of API/Polymer Physical Mixtures in CP Process Solvents

An excess of material was added to a glass tube with a capacity of 15 mL (Samco, Sheffield, UK) containing 3 mL of solvent. These vials were sealed and crimped and placed in a reciprocal shaking water bath (ThermoFisher Scientific, Waltham, MA, U.S.A) maintained at 25 ±1 °C and shaken at 100 cpm. After 72 h, 1 mL of the solution was filtered using a 0.45 mm PTFE filter (Fisherbrand, Waltham, MA, U.S.A) and diluted to an appropriate concentration in mobile phase before being analysed by HPLC (as detailed below). All consumables which came into contact with the undiluted suspension were pre-heated prior to use. This was carried out for three separate vials.

Prescreening Study for the CP Process

The co-precipitation prescreening study was carried out in 40 mL glass vials (Samco, Sheffield, UK) using a drug to polymer ratio of 30:70. ASDs were precipitated from different solvent/antisolvent systems at different solvent/antisolvent ratios. The optimised parameters were applied in larger scale studies in a 100 mL glass EasyMax™ reactor (Mettler Toledo, Greifense, Switzerland) agitated with an overhead stirrer at 600 rpm and cooled antisolvent held at -10°C or 10°C (for SIM and HCTZ systems, respectively). Material produced during the prescreening study was retained and used to determine the solubility of the CP material in the end point solvent system, which was subsequently used to determine the maximum theoretical yield of the CP process on a g/g basis.

Solubility of CP Systems in Solvent/Antisolvent mix

Excess amounts of the model systems from the CP process were placed for 2 h in the 100 mL glass reactor of an EasyMax™ filled with the solvent/antisolvent system at the temperature and stirring rate described above. After 2 h the samples were filtered through a 0.45 µm PTFE filter (Fisherbrand™, Waltham, MA, U.S.A.) and analysed by HPLC (procedure detailed below). For each system, approximately 12 mL of the filtered solution was placed on a previously weighed aluminium dish with a 43 mm diameter (Fisherbrand™, Waltham, MA, U.S.A.). The weight was recorded, and samples were left in the fumehood at ambient temperature to evaporate to constant weight. Dry aluminium dishes were weighed again to estimate the amount of solute in the solvent. Samples were analysed in triplicate.

Physical Mixtures (PMs)

Physical mixtures were prepared by mixing crystalline API and polymer with a spatula in the ratio corresponding to spray-dried and co-precipitated samples. For FTIR analysis a PM of amorphous API and polymer was prepared. The API was melted on a PC-400D hot plate (Corning, USA) in an aluminium dish at 272 °C for 4 minutes and 120 °C for 10 minutes for HCTZ and SIM respectively, immersed in liquid nitrogen and ground using an agate pestle and mortar, unless stated otherwise. The amorphous character of the API was confirmed by PXRD, after which it was mixed with the polymer in the required ratio.

Determination of Process Yield

The yield was calculated by dividing the obtained weight (g) of processed powder by the total weight (g) of components initially subjected to processing. ASDs were produced *via* SD or CP in triplicate for each system investigated.

Powder X-ray diffraction (PXRD)

Spray-dried and co-precipitated samples was analyzed by PXRD (Mini-Flex II, Rigaku™ Corporation, Japan) with Ni-filtered CuK α radiation (1.54 Å). Samples were analysed on a zero-background silicon sample holder in reflections mode and the tube voltage and current were 30 kV and 15 mA, respectively. The diffraction patterns were obtained for 2θ between 5 to 40° with a step scan rate 0.05° per second. Diffractograms were acquired once for each sample.

Modulated Differential Scanning Calorimetry (mDSC)

Samples were weighed, placed in standard aluminium pans with a single hole in the lid and analysed on a Q200 Differential Scanning Calorimeter (TA Instruments, Leatherhead, UK) using nitrogen as the purge gas (50 mL/min). Samples containing spray-dried or co-precipitated systems of HCTZ with polymer and SIM with polymer were heated over a temperature range of 0 °C to 270 °C and 20 °C to 200 °C, respectively. Additionally, before the thermal analysis, a drying cycle was performed on the SIM systems using the following sequence: the samples were heated up to 110 °C at 5 °C/min and held isothermally there for 10 minutes, then were ramped at 5 °C/min to 20 °C. The process modulation which allows separation of reversing and non-reversing heat flow events for HCTZ and SIM systems were set at 0.54 °C/40s and 0.8 °C/60s, respectively at a ramp rate of 5 °C/min.

Thermograms for the raw materials were obtained by heating samples from 0 °C to 270 °C, 20 °C to 200 °C and 0 °C to 150 °C for HCTZ, SIM and polymers, respectively. The API samples were then cooled to 0 °C at 20°C/min and heated up again to 270 °C (HCTZ) and 200 °C (SIM). The heating rate and modulation of the mDSC analysis was the same as above.

Results were analysed in the TA Universal Analysis software (TA Instruments, Leatherhead, UK). The T_g midpoints are reported, except for the T_g values used in the Gordon-Taylor equation, where T_g onset values were used. Each sample was analysed in triplicate.

Thermogravimetric Analysis (TGA)

Samples were placed in standard aluminium pans and thermally analysed on the Thermogravimetric Analyser (Q20, TA Instruments, Leatherhead, UK) using nitrogen as the purge gas (50 mL/min) by ramping the temperature at 10°C/min up to 300°C. The results were analysed in the TA Universal Analysis software (TA Instruments, Leatherhead, UK). Samples were analysed in duplicate.

Determination of True Density by Helium Pycnometry

An Accupyc II 1340 Pycnometer (Micromeritics Norcross, GA, U.S.A) was loaded with approximately 150 mg of the sample placed in a sample cup of 1 cm^3 capacity. The samples were purged with dry helium (99.995% purity) at an equilibration rate of 0.0050 psig/min. Samples were purged 10 times prior to analysis and all samples were analyzed in triplicate.

Bulk Density and Carr's Compressibility Index (CCI)

Bulk density (ρ_b) and tapped density (ρ_t) were determined as previously described.[47] Powdered samples were added to a graduated glass syringe of 1 mL volume with graduations of 0.01 mL. A known volume of powder was filled into the syringe and the weight of the filled powder was measured using a pre-tared analytical balance. The bulk density was calculated by dividing the mass of the powder by the volume. The tapped density of the powder was then determined by tapping the syringe onto a level surface from a 5 cm height. Once the volume reading was constant over 100 tap periods, the weight was measured again, and the density was calculated. Tapped density was calculated by dividing the mass of powder by the 'tapped' volume. All samples were analysed in triplicate. The Carr's Compressibility Index (CCI) was calculated using Equation 1.

$$\mathrm{CCI} = 100 \times \frac{(\rho_b - \rho_t)}{\rho_t} \qquad (1)$$

Attenuated Total Reflectance Fourier Transform Infrared Spectroscopy (FTIR)

IR spectra were obtained using a Spectrum 1 FT-IR Spectrometer (Perkin Elmer, Connecticut, U.S.A) equipped with a universal attenuated total reflectance and diamond/ZnSe crystal accessory. Spectra were collected as an average of 4 scans with a resolution of 4 cm^{-1} over a wavenumber range 4000 – 650 cm^{-1}. The baseline in each spectrum was corrected by PerkinElmer Spectrum IR v 10.6.0 software and all spectra were normalized to an absorbance of 1.0. Spectra were acquired once for each sample.

Determination of Drug Content by HPLC

The amount of spray dried or co-precipitated powder theoretically equivalent to approximately 12.5 mg of API was added to a 50 mL volumetric flask and made up to the mark with mobile phase. The solution was sonicated for 10 min to ensure the formulation was fully dissolved before being analysed by HPLC (Alliance, Waters, Santry, Ireland) with a 2695 Separations Module system and 2487 Dual

Wavelength detector (Waters, Santry, Ireland) which was used at wavelength 271 nm and 238 nm for HCTZ and SIM, respectively.

For HCTZ systems the mobile phase A (acetonitrile) and the mobile phase B (0.1 M phosphate buffer) at pH 2.8 were pumped in a composition of 20:80 at a flow rate of 1 mL/min at 20°C, giving a retention time of 5.5 min. A 150 × 4.6 mm Kinetex + Luna Omega C18 column was used (Phenomenex, Le Pecq, France) with 5µm particle size was used. For SIM systems the mobile phase A (acetonitrile) and the mobile phase B (0.1% (w/v) orthophosphoric acid in water) were pumped in a composition of 65:35 at the flow rate of 1 mL/min at 25°C giving a retention time of 7.7 minutes. The column used for SIM was a 250 mm × 4.6 mm Spherisorb C8 column with a particle size of 5µm (Waters, Milford, MA, USA).

Drug content was calculated by determining the area under the curve and comparing to the area under the curve of standards of known concentration. The range of the calibration curve for HCTZ and SIM was between 1 µg/mL and 100 µg/mL with regression coefficients (r^2) of 0.999 and 0.998, respectively.

Polymer Content Determination

The percentage of polymer content in the systems was determined by subtracting the percentage of the API as analysed by HPLC, and residual solvent (RSC) as analysed by TGA, from the total powder weight as given in Equation 2.

$$Polymer_{\%} = 100 - (API_{\%} + \mathrm{RSC}_{\%}) \qquad (2)$$

Particle Size

Particle size distributions of raw materials and processed systems were obtained using a Mastersizer 3000 laser diffraction instrument (Malvern Panalytical, Malvern, UK) with a dry powder dispersion accessory (Malvern Aero S) filled with approximately 0.1 g of powder. The obscuration limits were set at 0.1% and 10% in the Mastersizer 3000 software. The applied air pressure was 2 bar with a feed rate set at 50%. The particle size is reported in terms of d_{10}, d_{50} and d_{90} which represent the diameters corresponding to 10%, 50% and 90%, respectively of the cumulative undersize volume distribution. Measurements were performed in triplicate and analysed using Mastersizer 3000 software (Version 5.61).

Scanning Electron Microscopy

Images of obtained powders were taken with a Zeiss ULTRA plus Scanning Electron Microscope (Carl Zeiss AG, Jena, Germany) equipped with a secondary electron detector at 2 - 5 kV. Powder samples

were placed onto carbon tabs mounted on to aluminium pin stubs and sputter-coated with gold under vacuum prior to analysis. The images were taken at various magnifications in more than one region of the sample.

Physical Stability Study

Freshly prepared samples were placed in a chamber containing a saturated sodium chloride solution at 25 °C to maintain a relative humidity (RH) of 75%. Samples were taken after four weeks (T4) and analysed by mDSC, TGA, FTIR and PXRD. The storage conditions were monitored using a Sensirion SHT31 Temperature & Humidity Sensor Evaluation Module (Sensirion, Stäfa, Switzerland).

Statistical Analysis

The differences between powders prepared via both processes were analysed for statistical significance using a two sample Student t-test in Origin software (OriginLab, Massachusetts, USA). In all statistical analyses $p < 0.05$ denoted significance.

Results and Discussion

Identification of Model System Components

The intention of this work was to assess the process performance, physical properties, and stability of ASDs prepared *via* co-precipitation and compare them directly to ASDs produced by the more established spray-drying method. By focusing on APIs with different physicochemical characteristics and assessing the product yields, quality and stability, this work aims to provide insights that lead to being able to systematically identify the preferred route to generating ASDs based on the API properties. Two model drugs were used in this study: hydrochlorothiazide (HCTZ) and simvastatin (SIM). The main differences between these two compounds relate to their glass transition temperatures and the number of hydrogen bond donors and acceptors. The details of physicochemical properties of the two APIs are presented in Table 1. As shown, HCTZ has much a higher T_g and larger number of hydrogen bond acceptor and donor groups than SIM, which may influence the intermolecular interactions with polymeric excipients, homogeneity, and physical stability of the amorphous form of the drug.[48]

The polymers used to form ASDs in this work were selected based on the possible interactions between them and the API and also their physical properties. PVP/VA (poly(1-vinylpyrrolidone-co-vinyl acetate) consists of the hydrophilic monomer, vinylpyrrolidone (VP) and hydrophobic monomer, vinyl acetate (VA) in a 6:4 (VP:VA) ratio. The different monomers that make up the polymer contribute to different ASD properties, where the hydrophilic VP part of polymer generates supersaturation during dissolution of the ASD, while the hydrophobic VA monomer inhibits recrystallization from the supersaturated solution.[49] PVP/VA has also been reported to be less hygroscopic than PVP due to the exchange of some VP moieties for the more hydrophobic VA group.[50] Soluplus®, which is polyvinyl caprolactam–polyvinyl acetate–polyethylene glycol graft copolymer also exhibits amphiphilic properties where the hydrophilic part is comprised of polyethylene glycol and the lipophilic part comprises vinyl caprolactam and vinyl acetate.[51] The structures of the APIs and polymers are shown in Figure 1.

Comparison of HCTZ ASDs Produced by SD and CP

HCTZ CP Process Development

In contrast to SD (where process parameters for ASDs were available in the literature for similar HCTZ systems), CP is a more nascent approach that requires careful consideration with regard to process development. The choice of solvents used is crucial to the success of this approach. Solvents were selected by identifying commonalities between the solubilities of the API and polymer, meaning that solvents in which both components (API and polymer) would either dissolve very well or very poorly were chosen. On this basis, ethanol and hexane were chosen as a ‘good’ solvent and ‘poor’ solvent (antisolvent) pairing. Whilst the API and polymers have suitably low solubility in pure hexane, it was necessary to experimentally assess if this effect was maintained upon dilution with ethanol. The

equilibrium solubility of HCTZ from a physical mixture with a model polymer (Soluplus) in a 3:7 weight ratio in hexane was found to be <0.01 mg/mL (0.003 ± 0.003 mg/mL), whereas in a solvent mix with ethanol in the ratio 1:4 (EtOH:hexane) the equilibrium solubility increased to 0.09 ± 0.006 mg/mL. However, despite the 30 times increase in the equilibrium solubility after dilution with a good solvent (EtOH) for the API, the solubility of the physical mixture remained low.

The ASD solubility in the mixed solvent system establishes the maximum theoretical yield of the process, as the smaller the amount of the CP product that can be dissolved by the final solvent composition, the more of the material in the feed solution that can be recovered as CP ASD. In the context of process development, increasing solubility in the binary solvent mixture might have a significant negative impact on process yield and potentially slow down the precipitation kinetics to the point where the API is able to crystallise. At the same time, minimising the amount of ethanol introduced to the antisolvent limits the rate of addition of API and polymer which has a corresponding effect on the productivity of the process. This gives rise to a possible trade-off between the quality of the product and the efficiency of the process. To begin to address this, preliminary screening experiments aimed at optimizing the process were performed to determine the solubility of the model ASD formulation composition as well as dissolved API content from the ASD in a solvent mix at different solvent/antisolvent (S/AS) ratios and process temperatures. The solubility of the model polymer (Soluplus®) was also compared to the solubility of the ASD under the same conditions in order to evaluate the precipitation potential. It was observed that the polymer solubility was reduced when mixed with the less soluble API at a molecular level in the ASD. Results of these preliminary studies are provided in Table 2.

The increase in S/AS ratio (from 1:3 to 1:4) resulted in approximately 3.8 times decrease in the solubility of the model CP system at the same temperature (10°C), from 2.24 mg/g to 0.63 mg/g, which was also associated with an increase in yield from approximately 47.9% to 62.7%. No difference in yield was observed during the pre-screening studies when the temperature was altered between 5 °C and 10 °C. Based on the solubility of the powders (mg/g of the solvent mix) the process conditions were selected to be 10 °C and 1:4 solvent to antisolvent ratio. The solubility of the aforementioned model system was investigated under these conditions resulting in a theoretical maximum yield of 95.9%.

CP and SD Process Comparison

Table 3 shows the yields obtained from the SD and CP processes. In all cases, the CP yields are much lower than the maximum theoretical value. This is not surprising as divergence between theoretical and achieved yields are typical for experiments of this nature on a small scale with small losses in powder at different unit operations of the process accounting for a significant percentage of observed yield loss. To verify this explanation for the discrepancy, the ASD content of the mother

liquor and reaction vessel walls (redissolved in 100 mL of ethanol) for the co-precipitated system containing Soluplus® and 30% w/w API were determined. These were found to be 0.0002 ± 0.0001 g/g and 0.005 ± 0.001 g/g solvent mixture for the mother liquor and reaction vessel, respectively. This accounts for approximately 4% of the divergence between the obtained yields presented in Table 3 and the yield estimated from material loss in the mother liquor and material left in the vessel. Additional losses were assumed to have occurred while handling the powder during the filtering, drying and grinding steps.

In the examples presented here, the yields for equivalent SD and CP systems are very similar, with no statistically significant difference between the two. Yields for the SD products are similar to what are typically expected. Despite the greater variability in the CP yields, the process might be seen as more promising than SD in this respect as it is far from optimised and so has the potential to outperform SD if developed further at larger scales of production where solids handling based loses ('physical losses') would be anticipated to be far less significant than at the 1 g scale isolation conducted here. However, the 'theoretical losses' derived from the solubility of the co-precipitated powders in the mother liquor under studied conditions should remain the same at a larger scale, resulting in a theoretical maximum yield of 95.9%.

As can be seen in Table 3, the intended API to polymer ratio was achieved for both CP and SD processes. This is not normally considered to be a potential problem when spray drying as the feed solution and droplets are assumed to be homogeneous. However, there is the possibility that during co-precipitation the polymer and API precipitate at different rates, leading to the powder containing the incorrect API:polymer ratio and consequently a poorer quality and less stable product. Further work is required to understand the limits of the process in this regard, however the data suggests there is no reason to choose SD over CP or vice versa in terms of the process performance and product composition. The comparison of total solvent systems volumes required for SD and CP samples to yield a 1 g of a dry powder is presented in Table 3 (assuming the spray dryer is running at steady state). For each of the equivalent CP and SD systems approximately three times the solvent volumes are needed to obtain 1 g of a dry product in the CP process compared to SD. In terms of solvent cost and organic solvent waste the SD technique seems to be a superior one, however again, this large difference might be due to the relative inefficiency of co-precipitation conducted at small scale.

Physicochemical Characteristics of HCTZ Systems

The amorphous nature of all the samples produced by SD and CP was confirmed by PXRD analysis after their preparation and compared to the diffractograms of physical mixtures (PMs) containing polymer and crystalline API (Figure 2). It was determined experimentally by examining PMs with different API loadings that the PXRD is able to detect as low as 5% (w/w) of crystalline HCTZ in a formulation.

A single T_g was observed in each of the SD and CP freshly prepared samples. Even if both components remain amorphous, it is possible that the drug will not be soluble in the polymer at high

drug:polymer ratios which can result in amorphous-amorphous phase separation and can result in subsequent recrystallization of the API. The system may be described as homogenous if there is only one T_g observed by DSC.

The T_gs of the amorphous form of the pure components were assessed experimentally (mDSC thermograms are show in Figure S2). For melt-quenched HCTZ, Kollidon VA 64 and Soluplus® the midpoint T_g values were 116 ± 1.0 °C, 107 ± 0.8 °C and 69 ± 0.9 °C, respectively. The melting point of HCTZ was determined to be 271 ± 0.3 °C. The T_g midpoints of freshly prepared formulations with CP and SD systems with HCTZ and polymers are shown in Table 4.

The two different processes resulted in products with statistically significant differences in the T_g values of the ASDs. This suggests that there are differences in the strength of the interactions between drug and polymer in the products produced by SD and CP. To ascertain the extent of intermolecular interactions in the spray dried and co-precipitated systems, the Gordon-Taylor (G-T) model was used to predict ideal T_gs which were then compared to experimental values. The G-T model presumes no specific drug-polymer interactions. Divergences between predicted and experimental T_g values can signal interactions between components, as deviations from the predicted values stem from the non-ideal mixing of drug and polymer.[52] The G-T equation,[53] Eq. (3), predicts the values of T_gs of solid dispersions based on the respective T_g values of the individual components, their weight fraction in the ASD and their (amorphous) density. In Eq. (3) T_{g1} is the onset glass transition temperature of the polymer (100.0 ± 1.1 °C for PVP/VA and 63.0 ± 1.0 °C for Soluplus®), w_1 is the weight fraction of the polymer, T_{g2} is the onset glass transition temperature of the API (111.0 ± 0.9 °C for HCTZ), w_2 is weight fraction of the API. The parameter *K* was calculated by the Simha-Boyer rule,[54] Eq. (4), where the *K* parameter is calculated from the onset T_gs and densities (ρ) of the amorphous components, where ρ_1 is the true density of the polymer and ρ_2 is the true density of the API. The true density (ρ) values were determined using helium pycnometer and are as follows: 1.22 ± 0.04 g/cm^3 for PVP/VA, 1.17 ± 0.07 g/cm^3 for Soluplus®, and 1.72 ± 0.02 g/cm^3 for crystalline HCTZ. It was difficult to obtain melt quenched HCTZ in the minimum amount necessary for the helium pycnometer cell, as its degradation temperature is close to its melting point. The amorphous form density was therefore calculated based on previous reports where, for other APIs, it was shown to be 5% lower than that of the crystalline form.[55,56] This was applied to both APIs investigated in the current study to retain uniformity in the approach. The density of amorphous HCTZ used in calculations of composite T_gs was taken to be 1.63 g/cm^3.

$$T_{g,mix} = \frac{w_1 T_{g1} + K w_2 T_{g2}}{w_1 + K w_2} \qquad (3)$$

$$K = \frac{T_{g1}\rho_1}{T_{g\,2}\rho_2} \qquad (4)$$

Figure 3 shows a significant positive deviation from the predicted values for both SD and CP ASDs with both polymers. A similar positive deviation was previously reported for several combinations of spray dried thiazides (including HCTZ) with PVP.[57] Positive deviations were associated with hydrogen bond formation between API and polymer and a greater deviation from the G-T predicted values is suggestive of stronger interactions between API and polymer. For the Soluplus® systems this suggests that ASD formation by SD is more favourable in this respect as stronger hydrogen bonding can result in better physical stability of the amorphous API form.[58-59] The difference in deviation is less pronounced between CP and SD when PVP/VA is used as the stabilising polymer. For both polymers, the strength of the interactions between the components has a synergistic effect on the T_g of the ASD (i.e. the T_g of the ASD is higher than that of either pure component). In the case of PVP/VA systems, the influence of the processing method is potentially masked by the strength of the intermolecular bonds.

To verify these findings, FTIR analysis was performed on the samples (Figure 4 A and B) as the presence of shifts in the spectra can be indicative of hydrogen bonding between polymer and API. Additionally, differences in the spectra of crystalline and amorphous melt-quenched HCTZ were observed. In the crystalline form of HCTZ, the spectrum shows three sharp peaks at 3359 cm^{-1}, 3260 cm^{-1} and 3165 cm^{-1}, which correspond to the amine group (N-H). In the spectra of the amorphous melt-quenched HCTZ and its physical mixtures with both polymers the peak at 3165 cm^{-1} is no longer visible and the two other peaks are less intense. The aforementioned peaks are no longer visible in SD and CP samples which may signify that they have shifted downwards and are hidden behind C-H stretching peaks from 3020 to 2804 cm^{-1} due to hydrogen bonding between API and polymer in the processed systems. The peaks characteristic of the carbonyl groups (C=O) present in both polymers are between 1730 to 1600 cm^{-1}. In SD and CP systems with PVP/VA the peaks in this region are more intense than for the PM, which might also indicate hydrogen bond formation with the API hydrogen bond donors – amine groups (primary or secondary). In SD and CP systems with Soluplus® the peaks are split at 1606 cm^{-1} indicating hydrogen bonding between the carbonyl group of the polymer and API donor group, which was not observed at the peak of 1600 cm^{-1} in the PMs. The absence of the split peak in the PM spectra and its presence in the spectra of the processed samples can be attributed to the intermolecular interactions between Soluplus®, hydroxyl (OH) donor group and sulfonyl acceptor groups (O=S=O) of HCTZ. The split in the peak for systems with Soluplus® has been previously reported for spray dried materials, where it indicated hydrogen bond formation[60]. The observed shifts in the FTIR spectra signify hydrogen bond formation between HCTZ and both polymers, which is in agreement with the positive deviations for predicted values obtained with the G-T equation. As the shifts are identical for ASDs produced by SD and CP, the interactions between the functional groups can also be assumed to be independent of processing method.

Particle Size, Morphology and Flow Characteristics

The CP particles were significantly larger than SD particles and the d_{10}, d_{50} and d_{90} values, which agree with the SEM results, can be found in Table 5. The factors governing the particle size for powders produced by spray drying are well understood, however the same cannot yet be said for co-precipitated powders. The particle size is likely a function of a combination of factors such as shear forces in solution, solid content, feed rate, nozzle diameter, antisolvent temperature and solution viscosity.[30] Differences in particle morphologies and porosity may influence the bulk densities, flowability, and downstream processing of powders.[34,32] The SEM images of SD samples showed agglomerates generated from the primary particles, but these were not visible in the images of the CP systems. Both SD and CP samples were comprised of irregularly shaped particles, with SD samples forming shrivelled particles (Figure 5). The SEM images confirmed the larger particle size and higher porosity (Figure S3) of co-precipitated ASDs compared to analogous spray dried powders, in line with the study of Hou *et al*.[32] and similar images of co-precipitates generated from organic solvents and aqueous soluble polymers were presented in the study of Schenck *et. al*.[61]

Large particles are advantageous for downstream formulation processes, however high porosity and ensuing low bulk density are less desirable traits. A recent report has shown that this can easily be addressed in-line by washing the co-precipitate with hot antisolvent during filtration which causes the porous structure to collapse without the API-recrystallising.[31] Bulk density, tapped density and Carr's Compressibility Index (CCI) are presented in Table 6. Despite the differences in particle size of SD and CP powders, the bulk density was not significantly different for almost all systems. The only difference was found for the HCTZ-Soluplus® systems containing 40% (w/w) HCTZ, for which the CP material had a higher bulk density than the equivalent SD system ($p=0.0053$). The CCI indicates the flowability properties of powders based on their bulk and tapped densities. A powder's ability to flow easily is sought in drug product manufacture to provide a smooth flow into direct compression dies and allow consistency of content, weight, and hardness. The co-precipitated HCTZ-Soluplus® system containing 40% (w/w) HCTZ was the only one which could be categorised as having "passable flow" (with a CCI less than 26%), while all other powders were categorised as 'poorly flowable' (CCI of 26-31%) or 'very poorly flowable' (CCI of 32-37%) based on their CCI.[62] The aforementioned porosity of the HCTZ CP systems is a possible factor in the poor flowability of the larger particles.

Co-precipitation facilitates facile manipulation of powder properties through the formation of multicomponent particles. Incorporating other excipients alongside the stabilising polymer has been shown to improve the dissolution rate and powder handling characteristics.[33] Particle engineering by means of co-precipitation-based approaches therefore represents a potential route to drug product manufacture where previous attempts using ASDs produced by spray drying have been unsuccessful. Improved flowability of CP materials can also be achieved by downstream processing of the materials such as densification by means of solvent wash processes.[34]

Stability Study

The HCTZ CP and SD systems remained amorphous (PXRD shown in Figure S4, mDSC thermograms are show in Figure S5) after four weeks (T4) at 25 °C and 75% RH and were subsequently analysed by mDSC, TGA and FTIR. Both SD and CP powders were visually assessed at the beginning and end of the physical stability study. No changes were observed, with the powders remaining white with no visible differences in colour or morphology (data not shown). After four weeks on storage, the thermograms for all systems showed a single T_g, indicating that no phase separation had yet occurred. As shown in Table 7, the storage conditions during the stability study did not result in a decrease in T_g of the systems with HCTZ. While only the T_g of the co-precipitated ASD containing Soluplus® and 40% API was significantly different from that of the fresh sample (p=0.01) presented above in Table 4, the standard deviations of the T_gs for all systems prepared with this polymer were larger than in the systems with PVP/VA. The moisture content absorbed on storage was comparable to the other systems, however, for powders with Soluplus® the effect of moisture uptake on the T_gs over a period longer than 4 weeks under the same conditions may be merited, as the larger deviations in T_g might suggest the beginnings of a heterogenous system.

The influence of the stability study conditions on the intermolecular interactions between API and polymer functional groups was investigated by FTIR, as it was previously reported by Rumondor *et al.* that moisture sorption had an effect on drug -polymer interactions.[63] As presented in the Figure 6A, there was only minimal shift observed for all the systems from 1661 cm^{-1} at T0 to 1659 cm^{-1} at T4, characteristic for the carbonyl group (C=O) of the PVP/VA. Both SD and CP systems seem to retain the API-polymer interactions. The sharp peaks characteristic of the amine groups of crystalline HCTZ in the region 3359 – 3165 cm^{-1} were not observed in any of the processed systems investigated. Furthermore, the broad band characteristic for this region in the amorphous systems remained downshifted in most of the systems, indicating the possibility of hydrogen bond formation with the acceptor group of the polymers (carbonyl group). The spray-dried system with Soluplus® with an API loading of 30% (w/w) and coprecipitated system with an API loading of 40% (w/w) showed more noticeable broad bands in this region in Figure 6B.

In Figure 6B instead of the split at the top of the peak at 1599 cm^{-1} attributable to the carbonyl group (C=O) of the Soluplus®, the band was slightly shifted or absent in the spectra of both of the ASDs produced by SD and the co-precipitated ASD containing 40% API. These changes may signify a decrease in interactions between API and polymer. No changes were found between SD and CP systems with PVP/VA at T4. As described, there are changes in the spectra of systems with Soluplus® between T0 and T4, however they are relatively similar for both SD and CP samples. The choice of manufacturing technique seems to be irrelevant in terms of the stability of the intermolecular interactions in the systems with PVP/VA, where T4 spectra were comparable to equivalent T0 spectra. Systems with Soluplus®, while showing large variation of T_g (Table 7) which possibly indicates the start of physical changes in the systems such as amorphous-amorphous phase separation, also showed some decline in intermolecular bonding, based on differences in FTIR spectra for both SD and CP samples. Longer term stability studies are required to determine if these changes will ultimately lead to recrystallization of the API.

Comparison of SIM ASDs Produced by SD and CP

SIM CP Process Development

As was the case for HCTZ, a pre-screening study for the CP SIM process was performed in order to identify a suitable solvent/antisolvent system for the CP. As SIM exhibits excellent solubility in most common organic solvents,[64] solvent system selection proved to be more challenging than for HCTZ. For example, when the same ethanol/hexane system used for HCTZ was used to co-precipitate SIM ASDs no product was recovered. DCM/hexane was identified as a suitable solvent/antisolvent system for the CP process, however a pre-screening study found that solvent: antisolvent ratio of 1:30 was required to achieve co-precipitation (Table 8). The calculated theoretical maximum yield of the process based on the amount of solvent used, product dissolved and total solid content in grams was estimated to be at 90.9%. The high amounts of solvent required for CP imply that when the API (or polymer) are highly soluble in organic solvents, then SD is preferable from a process intensification point or that other supersaturation generation methods such as pH swing or salting out should be investigated as an alternate to solvent anti-solvent approaches used here to compare CP and SD solvent based production methodologies.

CP and SD Process Comparison

The compositions and yields for SIM ASDs produced by spray drying and co-precipitation are shown in Table 9. Products from SD and CP contained comparable amounts of API which were close to the intended value and so there is no evidence that one process is more advantageous over the other in terms of API lost during formulation processing.

The yields of the SD ASDs were significantly higher than for the corresponding CP ASDs in all cases and were also higher than yields of SD HCTZ ASDs. The improvement in SD yield for the SIM ASDs is attributed to the higher total solid content in the feed solution, which also generally leads to the larger particle size of the SD products for SIM relative to the SD HCTZ ASDs (Table 5). At the same time, the particle size of the SIM CP products was smaller than that of the HCTZ co-precipitates, leading to greater difficulty in recovering the powder and higher losses during filtration and drying steps. The concentration of the system with 30% w/w of SIM and Soluplus® in the mother liquor after filtration was gravimetrically evaluated and found to be 0.9 ± 0.1 mg/g of solvent mixture and more amount of powder was lost to the vessel walls and stirring blade (4.0 ± 0.1 mg/g) (the residue in the vessel having been redissolved in 100 mL of ethanol). It was estimated that the remaining approx. 5% of the yield mass balance was lost during filtering, drying and grinding processes.

In spite of the higher solubility of the SIM ASD components in the CP process solvent/antisolvent system, the yields of co-precipitated SIM and HCTZ systems are comparable. This suggests that, at this scale, the dominant factor in determining the yield is the geometry of the setup, as opposed to the

thermodynamics and kinetics of the co-precipitation process itself. Despite, the losses of powder related to its solubility and handling at a small scale (1 g) being similar for both molecules, the theoretically calculated losses for the APIs were different, with the ones for SIM being larger. As discussed earlier, this implies that yields for CP are likely to improve as the process is scaled up to clinical and commercial production scale and become closer to the maximum thermodynamic yield. However, if working at smaller scale and a high yield is required, SD is preferable for ASD formation rather than CP.

The differences in the solvent demand for the two processes are even more evident for the SIM systems than for HCTZ. Owing to SIM's excellent solubility in organic solvents and the high ratio of antisolvent required to obtain a product, the amount of solvent required to produce 1 g of a dry powder by CP is approximately 6 times higher than the amount used for SD. If solvent recycling and reuse is not considered, the much larger solvent volume necessary to obtain coprecipitated product also highlights the SD method as a superior technique.

Physicochemical Characteristics of SIM Systems

All ASDs produced by SD and CP were found to be amorphous by PXRD immediately after preparation (Figure 7). The amorphous nature was confirmed by mDSC analysis, which yielded thermograms (Figure S6) with a single T_g (Table 10).

The only CP and SD systems with statistically significantly different T_g values ($p = 0.0001$) were the samples containing PVP/VA and 40% w/w SIM. The slightly higher T_g of the CP product could be an indication of slightly stronger interactions between SIM and PVP/VA. The Gordon-Taylor equation (Eq 3) with Simha-Boyer rule (Eq. 4) was used here to predict the T_g of composite systems (Figure 8). The onset T_g for SIM was 29.5 ± 0.2 °C and the measured true density of crystalline SIM was 1.73 ± 0.04 g/cm^3, giving a calculated true density for the amorphous form of 1.64 g/cm^3. The true density values used for the polymers were the same as for the HCTZ model, and based on a different thermal method used, T_g onset of 65.7°C for Soluplus and 99.02°C for PVP VA 64 were applied. As the predicted values of SIM:PVP/VA64 were close to the theoretically obtained ones, the confidence interval curves showing the positive and negative error were added based on the standard deviations of the experimental values.

Both PVP/VA and Soluplus®-based ASDs deviated negatively from the predicted values. This deviation is more pronounced for the ASDs containing Soluplus® compared to PVP/VA systems. SIM is reported to form dimers through homomolecular interactions which restricts its ability to form intermolecular bonds with the polymer.[65] A lack of drug-polymer interactions may lead to increased molecular mobility, resulting in a decrease in drug stability and a greater risk of API recrystallization. The negative deviation suggests that homomolecular interactions may be superior to the heteromolecular interactions between the two components of the ASD, which in turn may have a destabilizing effect on the ASDs.[52]

To investigate this further, the FTIR spectra of SD and CP samples, crystalline SIM, amorphous SIM and its physical mixtures with polymers were obtained (Figure 9A and B). The characteristic peak at 3547 cm^{-1} attributed to OH stretching that is seen in the spectrum of amorphous SIM is much broader than that found in the spectrum of the crystalline form of SIM, as was also noted in the study by Ambike *et. al.*[66] In the spectra of all the processed samples and PMs this peak is no longer present or it appears as a broad band which might indicate weak intermolecular bond formation between SIM and polymers in the ASDs. There are also shifts observed in the region characteristic for the carbonyl group (C=O) for all the systems at 1631 cm^{-1} and 1660 cm^{-1}. It is difficult to confirm that the small shifts visible on the spectra are due to the self-association of SIM. Kapourani *et al.* also described a negative deviation from the GT predicted values for SIM-PVP systems prepared by quench-cooling. However, as reported by those authors, it was not possible to determine whether the negative deviation is correlated to the SIM-SIM interactions, as the FTIR shifts in the region of 3700–3000 and 1600–1800 cm^{-1} can be attributed to both homo and hetero-molecular interactions.[65] As the same observation was made with respect to a negative deviation from predicted T_g values for ASDs produced by both SD and CP, there is no apparent benefit of choosing one process over the other to encourage more favourable intermolecular interactions between API and polymer when the API is prone to forming homomolecular bonds.

Particle Size, Morphology and Flow Characteristics

The particle size values (d_{10}, d_{50}, d_{90}) for the SD and CP products are presented in Table 11. For SIM-containing ASDs, powders produced by CP are significantly larger than those prepared by SD which is in agreement with what was found for the HCTZ systems, indicating that it is possible to consistently generate large ASD particles with CP. The larger particle size of CP products is also evident in the SEM images in Figure 10.

While the bulk density of the co-precipitated powders was on average lower than the spray-dried systems (Table 12), their CCI values indicate better powder flowability. It is well known that finer particles are more affected by the attractive forces resulting in their cohesion, thus reducing flowability. SD systems could be categorised as having ‘passable’ (CCI of 26-31%) to ‘very poor’ flowability (CCI of 32-37%). In contrast, the CP systems with the larger particle size could be classified in the range of ‘fine’ to ‘passable’ flowability based on their CCI values.[62]

The SD SIM images show spherically shaped particles, whereas CP SIM co-processed samples are low aspect ratio irregularly shaped particles. The shape of CP systems is similar to the equivalent samples containing HCTZ, whereas the SD systems formed more spherical particles than those of HCTZ (Figure 5). Particle size and shape affect the flowability and compaction properties of the bulk powder (for example spherical particles are more prone to agglomeration) which in turn impacts the processability of the powder during formulation unit operations.[67] Whilst not investigated as part of the current work, powder property optimisation is likely a key consideration for process selection. Differences in particle morphology between spray dried SIM and HCTZ systems are likely due to a

combination of the differences in the total solute concentration and drying kinetics of the droplet, which are often described by the dimensionless Peclet number.[68] When the evaporation rate of the solvent on the surface is faster than the diffusion of the solutes to the centre of the droplet, the formation of a skin or shell on the surface results.[69] The hollow particle may shrivel or break after particle formation, as was observed for the spray dried HCTZ powder.

Stability Study

All samples remained amorphous when analysed by PXRD (Figure S7) and mDSC (Figure S8) after 4 weeks on stability. Images of the samples before (T0) and after the stability study (T4) in Figure 11 reveal important differences in the way that spray dried and co-precipitated ASDs behave on storage. Compared to fresh samples, the spray dried systems containing PVP/VA underwent significant changes in colour and bulk structure of the ASD from a powder to a hard gel-like entity. Interestingly, the images in Figure 11, show that the equivalent systems prepared by CP remained as a fine powder over the course of the experiment, however their change in colour from white to brown was noted. While the changes for the Soluplus®-based ASDs were not as extreme as for the PVP/VA systems, the spray dried samples showed a slight discolouration from white to yellow and the formation of larger aggregates was observed. Again, this is in contrast to the co-precipitated products, the physical characteristics of which appear to be unaffected by the storage conditions.

PVP/VA is reported to be more hygroscopic than Soluplus® [70] which may be responsible in part for these ASDs undergoing a more dramatic transition from white powder to a brown gel under the test conditions (25 °C, 75% RH). However, the moisture content of all the samples was comparable at the end of the study (Table 13) and so the observed differences in behaviour might stem from the larger size of the CP particles. A larger particle size is indicative of a lower specific surface area for the powder and so, while it is still able to absorb moisture, the water is not able to permeate as deeply into the particle structure, meaning the effects are confined to the surface material. Further work is required to investigate this, however this finding suggests that the physical stability of some ASDs can be improved by employing co-precipitation, the advantages of which may be more pronounced when using hygroscopic polymers.

A significant difference between T_gs at T0 and at T4 for all samples can be seen form the data presented in Table 13. An increase in the residual moisture content was apparent in all the systems, and was in the range of approximately 1.25 to 2.25%. While most systems absorbed comparable amounts of moisture, the spray-dried system with Soluplus® at the lower drug loading absorbed more than the equivalent coprecipitated one. Water is a well-known plasticiser and it is possible that in a highly humid environment the T_g of ASDs systems can be lowered to the point that the system becomes unstable and recrystallization occurs.[63] Neither the PXRD nor mDSC analysis showed any evidence of crystallisation despite the significant decrease in the system T_gs. However, increased moisture content can also result in a decrease in chemical stability which should also be evaluated as

part of future work before the stability of ASDs produced by CP can be perceived as superior to that of SD systems.

As with HCTZ, possible changes in the drug-polymer and drug-drug interactions at T4 relative to T0 were assessed by FTIR. At T4 the 3500-3200 cm^{-1} region, which is characteristic of the hydroxyl group stretching band of SIM, is more intense than at T0 for all the processed samples in the evaluated ATR-FTIR spectra (Figure 12). This change may signify that the hydrogen donor group in the API creates weaker bonds with the acceptor group of the polymer and other API molecules. Moreover, a shift of around 15 cm^{-1} in the 1900-1600 cm^{-1} carbonyl stretching peaks region was observed for all the systems with both polymers when the spectra at T4 were compared to those at T0. While these changes are consistent between co-precipitate and spray dried systems, the weaker interactions of the ASD components may affect the physical stability of the systems if the experiment was carried out over a longer period of time.

Conclusion

Evaluation of the characteristics of ASDs formed by antisolvent co-precipitation in this work has demonstrated it to be a valid approach for generating ASDs where a solvent based method is preferred. Spray drying and co-precipitation could be applied to both a high and low T_g model API, generating ASDs with similar solid state characteristics and solid state stability, and the choice of processing method seems to generally not impact on the solid state characteristics of the ASDs generated.

Co-precipitation may be seen as an advantageous approach in the systems with the low T_g API (SIM) and PVP/VA 64, as only a colour change was observed in those systems on stability, while more significant physical deterioration was observed for the equivalent spray dried systems. However, the high solubility of SIM in organic solvents meant that the process consumed large volumes of solvent, and so spray drying may be regarded as preferential until the co-precipitation process can be optimised. Similarly, at the small scales used for this work (c. 100 mL) significant amounts of the co-precipitated ASDs were lost to the surfaces of the equipment, resulting in yields of around 55-65% for all systems studied. In contrast, yields in excess of 80% were obtained for some of the spray dried products which indicates that spray drying is more productive at smaller scales. However, if co-precipitation scales in the same way as conventional crystallisation processes, yields can be expected to rapidly approach the maximum theoretical yield at higher volumes. The contrast in solvent demand in each of the two processes was stark for both drugs. Co-precipitation required three to six times the amount of solvent as spray drying to produce the same mass of product and so is another important consideration when choosing between the two processes.

One of the most obvious differences between the products of the two processes is the particle size, with the co-precipitates in this work being an order of magnitude larger that their spray dried

equivalents. Future work should be directed to add to understanding relationships between co-precipitation process parameters and particle size to enable highly engineered particles to be produced that would improve the powder properties of the ASD pertinent to downstream drug product manufacture (e.g. flowability, compactability), relative to those produced by spray drying. For SIM systems, CCI values indicated better powder flowability for the co-precipitated systems compared to equivalent spray dried systems, which is related to the differences in particle size and density of powders produced by the two different methods.

The present study has illustrated that co-precipitated and spray dried ASDs are almost identical on a molecular level in terms of their solid state interactions for two very different APIs, but also hints at the potential of employing co-precipitation to produce highly engineered particles. This latter aspect merits further investigation at larger scale.

Declaration of interests

The authors declare that they have no known competing financial interests or personal relationships that could have appeared to influence the work reported in this paper.

Acknowledgements

This work was supported by Science Foundation Ireland (SFI) 18/EPSRC-CDT/3587 and the Engineering and Physical Sciences Research Council EP/S023054/1. It was part funded by SFI and co-funded under the European Regional Development Fund 12/RC/2275.

Scanning Electron Microscopy images of obtained powders were taken at the Advanced Microscopy Laboratory (AML) (CRANN Institute, Dublin, Ireland).

References

1. Schenck, L.; Erdemir, D.; Saunders Gorka, L.; Merritt, J. M.; Marziano, I.; Ho, R.; Lee, M.; Bullard, J.; Boukerche, M.; Ferguson, S.; Florence, A. J.; Khan, S. A.; Sun, C. C., Recent Advances in Co-processed APIs and Proposals for Enabling Commercialization of These Transformative Technologies. *Molecular Pharmaceutics* **2020,** *17* (7), 2232-2244.
2. Shikha, S.; Lee, Y. W.; Doyle, P. S.; Khan, S. A., Microfluidic Particle Engineering of Hydrophobic Drug with Eudragit E100─Bridging the Amorphous and Crystalline Gap. *Molecular Pharmaceutics* **2022**.
3. Kalepu, S.; Nekkanti, V., Insoluble drug delivery strategies: review of recent advances and business prospects. *Acta Pharm Sin B* **2015,** *5* (5), 442-53.
4. Noyes, A.; Whitney, W., The rate of solution of solid substances in their own solutions. *J. Am. Chem. Soc* **1897,** (19), 930-934.
5. Savjani, K. T.; Gajjar, A. K.; Savjani, J. K., Drug solubility: importance and enhancement techniques. *ISRN Pharm* **2012,** *2012*, 195727.

6. Gupta, J.; Devi, A., Solubility EnhancementTechniques forPoorly Soluble Pharmaceuticals: A Review. *Indian Journal of Pharmaceutical and Biological Research* **2019,** *7*, 09-16.
7. Khadka, P.; Ro, J.; Kim, H.; Kim, I.; Kim, J. T.; Kim, H.; Cho, J. M.; Yun, G.; Lee, J., Pharmaceutical particle technologies: An approach to improve drug solubility, dissolution and bioavailability. *Asian Journal of Pharmaceutical Sciences* **2014,** *9* (6), 304-316.
8. Gokturk, S.; Caliskan, E.; Talman, R. Y.; Var, U., A study on solubilization of poorly soluble drugs by cyclodextrins and micelles: complexation and binding characteristics of sulfamethoxazole and trimethoprim. *ScientificWorldJournal* **2012,** *2012*, 718791.
9. Park, C.; Meghani, N. M.; Shin, Y.; Oh, E.; Park, J. B.; Cui, J. H.; Cao, Q. R.; Tran, T. T.; Tran, P. H.; Lee, B. J., Investigation of Crystallization and Salt Formation of Poorly Water-Soluble Telmisartan for Enhanced Solubility. *Pharmaceutics* **2019,** *11* (3).
10. Ainurofiq, A.; Putro, D.; Ramadhani, D.; Putra, G.; Do Espirito Santo, L., A review on solubility enhancement methods for poorly water-soluble drugs. *Journal of Reports in Pharmaceutical Sciences* **2021,** *10* (1), 137-147.
11. Buddhadev, S., Pharmaceutical Cocrystals-A Review †. *Proceedings* **2021,** *62*.
12. Jiang, L.; Sun, Y.; Lu, A.; Wang, X.; Shi, Y., Ionic Liquids: Promising Approach for Oral Drug Delivery. *Pharmaceutical Research* **2022**.
13. Tsolaki, E.; Stocker, M. W.; Healy, A. M.; Ferguson, S., Formulation of ionic liquid APIs via spray drying processes to enable conversion into single and two-phase solid forms. *International Journal of Pharmaceutics* **2021,** *603*, 120669.
14. Shamshina, J. L.; Rogers, R. D., Are Myths and Preconceptions Preventing Us from Applying Ionic Liquid Forms of Antiviral Medicines to the Current Health Crisis? *International Journal of Molecular Sciences* **2020,** *21* (17), 6002.
15. Hancock, B. C.; Zografi, G., Characteristics and significance of the amorphous state in pharmaceutical systems. *J Pharm Sci* **1997,** *86* (1), 1-12.
16. Lu, X.; Huang, C.; Li, M.; Skomski, D.; Xu, W.; Yu, L.; Byrn, S. R.; Templeton, A. C.; Su, Y., Molecular Mechanism of Crystalline-to-Amorphous Conversion of Pharmaceutical Solids from 19F Magic Angle Spinning NMR. *The Journal of Physical Chemistry B* **2020,** *124* (25), 5271-5283.
17. Iyer, R.; Petrovska Jovanovska, V.; Berginc, K.; Jaklic, M.; Fabiani, F.; Harlacher, C.; Huzjak, T.; Sanchez-Felix, M. V., Amorphous Solid Dispersions (ASDs): The Influence of Material Properties, Manufacturing Processes and Analytical Technologies in Drug Product Development. *Pharmaceutics* **2021,** *13* (10).
18. Shibata, Y.; Fujii, M.; Suzuki, A.; Koizumi, N.; Kanada, K.; Yamada, M.; Watanabe, Y., Effect of storage conditions on the recrystallization of drugs in solid dispersions with crospovidone. *Pharmaceutical Development and Technology* **2014,** *19* (4), 468-474.
19. Wolbert, F.; Fahrig, I. K.; Gottschalk, T.; Luebbert, C.; Thommes, M.; Sadowski, G., Factors Influencing the Crystallization-Onset Time of Metastable ASDs. *Pharmaceutics* **2022,** *14* (2).
20. Bhujbal, S. V.; Mitra, B.; Jain, U.; Gong, Y.; Agrawal, A.; Karki, S.; Taylor, L. S.; Kumar, S.; Tony Zhou, Q., Pharmaceutical amorphous solid dispersion: A review of manufacturing strategies. *Acta Pharm Sin B* **2021,** *11* (8), 2505-2536.
21. Guo, Z.; Boyce, C.; Rhodes, T.; Liu, L.; Salituro, G. M.; Lee, K. J.; Bak, A.; Leung, D. H., A novel method for preparing stabilized amorphous solid dispersion drug formulations using acoustic fusion. *Int J Pharm* **2021,** *592*, 120026.
22. Browne, E.; Charifou, R.; Worku, Z. A.; Babu, R. P.; Healy, A. M., Amorphous solid dispersions of ketoprofen and poly-vinyl polymers prepared via electrospraying and spray drying: A comparison of particle characteristics and performance. *International Journal of Pharmaceutics* **2019,** *566*, 173-184.
23. Hengsawas Surasarang, S.; Keen, J. M.; Huang, S.; Zhang, F.; McGinity, J. W.; Williams, R. O., Hot melt extrusion versus spray drying: hot melt extrusion degrades albendazole. *Drug Development and Industrial Pharmacy* **2017,** *43* (5), 797-811.
24. Strotman, N. A.; Schenck, L., Coprecipitated Amorphous Dispersions as Drug Substance: Opportunities and Challenges. *Organic Process Research & Development* **2022,** *26* (1), 10-13.
25. Harmonization ICf International Council for Harmonization. Q3C impurities: residual solvents R6: FDA. 2019.
26. Chea, J. D.; Christon, A.; Pierce, V.; Reilly, J. H.; Russ, M.; Savelski, M.; Slater, C. S.; Yenkie, K. M., Framework for Solvent Recovery, Reuse, and Recycling In Industries. In *Computer Aided Chemical Engineering*, Muñoz, S. G.; Laird, C. D.; Realff, M. J., Eds. Elsevier: 2019; Vol. 47, pp 199-204.

27. McGinty, J.; Chong, M. W. S.; Manson, A.; Brown, C. J.; Nordon, A.; Sefcik, J., Effect of Process Conditions on Particle Size and Shape in Continuous Antisolvent Crystallisation of Lovastatin. *Crystals* **2020,** *10* (10).
28. Pascual, G. K.; Donnellan, P.; Glennon, B.; Kamaraju, V. K.; Jones, R. C., Experimental and Modeling Studies on the Solubility of 2-Chloro-N-(4-methylphenyl)propanamide (S1) in Binary Ethyl Acetate + Hexane, Toluene + Hexane, Acetone + Hexane, and Butanone + Hexane Solvent Mixtures Using Polythermal Method. *Journal of Chemical & Engineering Data* **2017,** *62* (10), 3193-3205.
29. Morris, G.; Power, G.; Ferguson, S.; Barrett, M.; Hou, G.; Glennon, B., Estimation of Nucleation and Growth Kinetics of Benzoic Acid by Population Balance Modeling of a Continuous Cooling Mixed Suspension, Mixed Product Removal Crystallizer. *Organic Process Research & Development* **2015,** *19* (12), 1891-1902.
30. Zhang, J.; Liu, M.; Zeng, Z., The antisolvent coprecipitation method for enhanced bioavailability of poorly water-soluble drugs. *International Journal of Pharmaceutics* **2022**, 122043.
31. Frank, D. S.; Punia, A.; Fahy, M.; Dalton, C.; Rowe, J.; Schenck, L., Densifying Co-Precipitated Amorphous Dispersions to Achieve Improved Bulk Powder Properties. *Pharmaceutical Research* **2022**.
32. Hou, H. H.; Rajesh, A.; Pandya, K. M.; Lubach, J. W.; Muliadi, A.; Yost, E.; Jia, W.; Nagapudi, K., Impact of Method of Preparation of Amorphous Solid Dispersions on Mechanical Properties: Comparison of Coprecipitation and Spray Drying. *J Pharm Sci* **2019,** *108* (2), 870-879.
33. Schenck, L.; Mann, A. K. P.; Liu, Z.; Milewski, M.; Zhang, S.; Ren, J.; Dewitt, K.; Hermans, A.; Cote, A., Building a better particle: Leveraging physicochemical understanding of amorphous solid dispersions and a hierarchical particle approach for improved delivery at high drug loadings. *Int J Pharm* **2019,** *559*, 147-155.
34. Frank, D.; Schenck, L.; Koynov, A.; Su, Y.; Li, Y.; Variankaval, N., Optimizing Solvent Selection and Processing Conditions to Generate High Bulk-Density, Co-Precipitated Amorphous Dispersions of Posaconazole. *Pharmaceutics* **2021,** *13* (12).
35. Schenck, L.; Koynov, A.; Cote, A., Particle engineering at the drug substance, drug product interface: a comprehensive platform approach to enabling continuous drug substance to drug product processing with differentiated material properties. *Drug Development and Industrial Pharmacy* **2019,** *45* (4), 521-531.
36. Shaikh, R.; Singh, R.; Walker, G. M.; Croker, D. M., Pharmaceutical Cocrystal Drug Products: An Outlook on Product Development. *Trends in Pharmacological Sciences* **2018,** *39* (12), 1033-1048.
37. European Medicines Agency. Reflection paper on the use of cocrystals of active substances in medicinal products. Available at https://www.ema.europa.eu/en/documents/scientific-guideline/reflection-paper-use-cocrystals-active-substances-medicinal-products_en.pdf. Accessed July 10, 2022.
38. Caron, V.; Tajber, L.; Corrigan, O. I.; Healy, A. M., A Comparison of Spray Drying and Milling in the Production of Amorphous Dispersions of Sulfathiazole/Polyvinylpyrrolidone and Sulfadimidine/Polyvinylpyrrolidone. *Molecular Pharmaceutics* **2011,** *8* (2), 532-542.
39. Ousset, A.; Chavez, P.-F.; Meeus, J.; Robin, F.; Schubert, M. A.; Somville, P.; Dodou, K., Prediction of Phase Behavior of Spray-Dried Amorphous Solid Dispersions: Assessment of Thermodynamic Models, Standard Screening Methods and a Novel Atomization Screening Device with Regard to Prediction Accuracy. *Pharmaceutics* **2018,** *10* (1), 29.
40. Mann, A. K. P.; Schenck, L.; Koynov, A.; Rumondor, A. C. F.; Jin, X.; Marota, M.; Dalton, C., Producing Amorphous Solid Dispersions via Co-Precipitation and Spray Drying: Impact to Physicochemical and Biopharmaceutical Properties. *J Pharm Sci* **2018,** *107* (1), 183-191.
41. Mahmah, O.; Tabbakh, R.; Kelly, A.; Paradkar, A., A comparative study of the effect of spray drying and hot-melt extrusion on the properties of amorphous solid dispersions containing felodipine. *J Pharm Pharmacol* **2014,** *66* (2), 275-84.
42. Homayouni, A.; Sadeghi, F.; Nokhodchi, A.; Varshosaz, J.; Afrasiabi Garekani, H., Preparation and characterization of celecoxib dispersions in soluplus(®): comparison of spray drying and conventional methods. *Iran J Pharm Res* **2015,** *14* (1), 35-50.
43. Shah, N.; Sandhu, H.; Phuapradit, W.; Pinal, R.; Iyer, R.; Albano, A.; Chatterji, A.; Anand, S.; Choi, D. S.; Tang, K.; Tian, H.; Chokshi, H.; Singhal, D.; Malick, W., Development of novel microprecipitated bulk powder (MBP) technology for manufacturing stable amorphous formulations of poorly soluble drugs. *Int J Pharm* **2012,** *438* (1-2), 53-60.
44. Hu, Q.; Choi, D. S.; Chokshi, H.; Shah, N.; Sandhu, H., Highly efficient miniaturized coprecipitation screening (MiCoS) for amorphous solid dispersion formulation development. *International Journal of Pharmaceutics* **2013,** *450* (1), 53-62.

45. Frank, D. S.; Prasad, P.; Iuzzolino, L.; Schenck, L., Dissolution Behavior of Weakly Basic Pharmaceuticals from Amorphous Dispersions Stabilized by a Poly(dimethylaminoethyl Methacrylate) Copolymer. *Molecular Pharmaceutics* **2022,** *19* (9), 3304-3313.
46. Mettler Toledo, Stirrers for 100 mL 2-Piece Reactors. Available at https://www.mt.com/my/en/home/products/L1_AutochemProducts/Chemical-Synthesis-and-Process-Development-Lab-Reactors/Synthesis-Reactor-Systems/EasyMax-Stirrers-for-100-mL-2-piece-reactors.html. Accessed December 20, 2022.
47. Healy, A. M.; McDonald, B. F.; Tajber, L.; Corrigan, O. I., Characterisation of excipient-free nanoporous microparticles (NPMPs) of bendroflumethiazide. *European Journal of Pharmaceutics and Biopharmaceutics* **2008,** *69* (3), 1182-1186.
48. Shi, Q.; Chen, H.; Wang, Y.; Wang, R.; Xu, J.; Zhang, C., Amorphous Solid Dispersions: Role of the Polymer and Its Importance in Physical Stability and In Vitro Performance. *Pharmaceutics* **2022,** *14*, 1747.
49. Knopp, M. M.; Nguyen, J. H.; Mu, H.; Langguth, P.; Rades, T.; Holm, R., Influence of Copolymer Composition on In Vitro and In Vivo Performance of Celecoxib-PVP/VA Amorphous Solid Dispersions. *AAPS J* **2016,** *18* (2), 416-23.
50. Taylor, L. S.; Langkilde, F. W.; Zografi, G., Fourier transform Raman spectroscopic study of the interaction of water vapor with amorphous polymers. *J Pharm Sci* **2001,** *90* (7), 888-901.
51. Shamma., R. N., ,; Basha., M., Soluplus®: A novel polymeric solubilizer for optimization of Carvedilol solid dispersions: Formulation design and effect of method preparation. *Powder Technology* **2013,** *237*, 406-414.
52. Baghel, S.; Cathcart, H.; O'Reilly, N. J., Polymeric Amorphous Solid Dispersions: A Review of Amorphization, Crystallization, Stabilization, Solid-State Characterization, and Aqueous Solubilization of Biopharmaceutical Classification System Class II Drugs. *J Pharm Sci* **2016,** *105* (9), 2527-2544.
53. Gordon, M.; Taylor, J. S., Ideal Copolymers and the Second-Order Transitions of Synthetic Rubbers. I. Noncrystalline Copolymers. *Rubber Chemistry and Technology* **1953,** *26* (2), 323-335.
54. Simha, R.; Boyer, R. F., On a General Relation Involving the Glass Temperature and Coefficients of Expansion of Polymers. *Journal of Chemical Physics* **1962,** *37*, 1003-1007.
55. Van den Mooter, G.; Wuyts, M.; Blaton, N.; Busson, R.; Grobet, P.; Augustijns, P.; Kinget, R., Physical stabilisation of amorphous ketoconazole in solid dispersions with polyvinylpyrrolidone K25. *Eur J Pharm Sci* **2001,** *12* (3), 261-9.
56. Browne, E.; Worku, Z. A.; Healy, A. M., Physicochemical Properties of Poly-Vinyl Polymers and Their Influence on Ketoprofen Amorphous Solid Dispersion Performance: A Polymer Selection Case Study. *Pharmaceutics* **2020,** *12* (5).
57. Tajber, L.; Corrigan, O. I.; Healy, A. M., Physicochemical evaluation of PVP-thiazide diuretic interactions in co-spray-dried composites--analysis of glass transition composition relationships. *Eur J Pharm Sci* **2005,** *24* (5), 553-63.
58. Janssens, S.; Van den Mooter, G., Review: physical chemistry of solid dispersions. *J Pharm Pharmacol* **2009,** *61* (12), 1571-86.
59. Kothari, K.; Ragoonanan, V.; Suryanarayanan, R., The Role of Drug–Polymer Hydrogen Bonding Interactions on the Molecular Mobility and Physical Stability of Nifedipine Solid Dispersions. *Molecular Pharmaceutics* **2015,** *12* (1), 162-170.
60. Kelleher, J. F.; Gilvary, G. C.; Madi, A. M.; Jones, D. S.; Li, S.; Tian, Y.; Almajaan, A.; Senta-Loys, Z.; Andrews, G. P.; Healy, A. M., A comparative study between hot-melt extrusion and spray-drying for the manufacture of anti-hypertension compatible monolithic fixed-dose combination products. *Int J Pharm* **2018,** *545* (1-2), 183-196.
61. Schenck, L.; Boyce, C.; Frank, D.; Koranne, S.; Ferguson, H. M.; Strotman, N., Hierarchical Particle Approach for Co-Precipitated Amorphous Solid Dispersions for Use in Preclinical In Vivo Studies. *Pharmaceutics* **2021,** *13* (7).
62. Pharmacopeia B. 2019. Appendix XVII N. Powder Flow. British Pharmacopeia.
63. Rumondor, A. C.; Wikstrom, H.; Van Eerdenbrugh, B.; Taylor, L. S., Understanding the tendency of amorphous solid dispersions to undergo amorphous-amorphous phase separation in the presence of absorbed moisture. *AAPS PharmSciTech* **2011,** *12* (4), 1209-19.
64. Oh, D.-J.; Lee, B.-C.; Hwang, S.-J., Solubility of Simvastatin and Lovastatin in Mixtures of Dichloromethane and Supercritical Carbon Dioxide. *Journal of Chemical & Engineering Data* **2007,** *52* (4), 1273-1279.
65. Kapourani, A.; Chatzitheodoridou, M.; Kontogiannopoulos, K. N.; Barmpalexis, P., Experimental, Thermodynamic, and Molecular Modeling Evaluation of Amorphous Simvastatin-Poly(vinylpyrrolidone) Solid Dispersions. *Mol Pharm* **2020,** *17* (7), 2703-2720.

66. Ambike, A. A.; Mahadik, K. R.; Paradkar, A., Spray-dried amorphous solid dispersions of simvastatin, a low tg drug: in vitro and in vivo evaluations. *Pharm Res* **2005,** *22* (6), 990-8.
67. Worku, Z. A.; Kumar, D.; Gomes, J. V.; He, Y.; Glennon, B.; Ramisetty, K. A.; Rasmuson, Å. C.; O'Connell, P.; Gallagher, K. H.; Woods, T.; Shastri, N. R.; Healy, A.-M., Modelling and understanding powder flow properties and compactability of selected active pharmaceutical ingredients, excipients and physical mixtures from critical material properties. *International Journal of Pharmaceutics* **2017,** *531* (1), 191-204.
68. Sadek, C.; Schuck, P.; Fallourd, Y.; Pradeau, N.; Le Floch-Fouéré, C.; Jeantet, R., Drying of a single droplet to investigate process–structure–function relationships: a review. *Dairy Science & Technology* **2015,** *95* (6), 771-794.
69. Boel, E.; Koekoekx, R.; Dedroog, S.; Babkin, I.; Vetrano, M. R.; Clasen, C.; Van den Mooter, G., Unraveling Particle Formation: From Single Droplet Drying to Spray Drying and Electrospraying. *Pharmaceutics* **2020,** *12* (7).
70. Patel, N. G.; Serajuddin, A. T. M., Moisture sorption by polymeric excipients commonly used in amorphous solid dispersion and its effect on glass transition temperature: I. Polyvinylpyrrolidone and related copolymers. *International Journal of Pharmaceutics* **2022,** *616*, 121532.

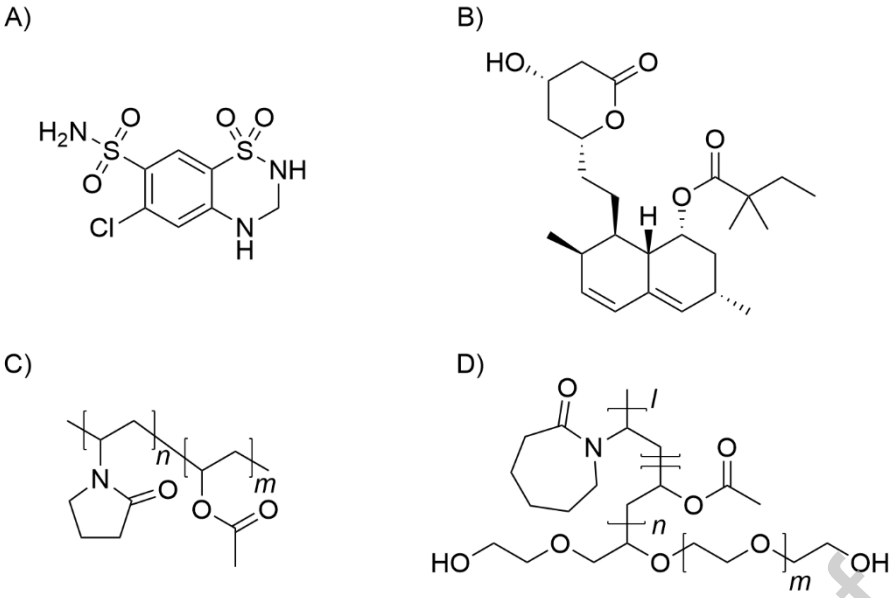

Figure 1. Chemical structures of A) Hydrochlorothiazide B) Simvastatin C) PVP/VA D) Soluplus®.

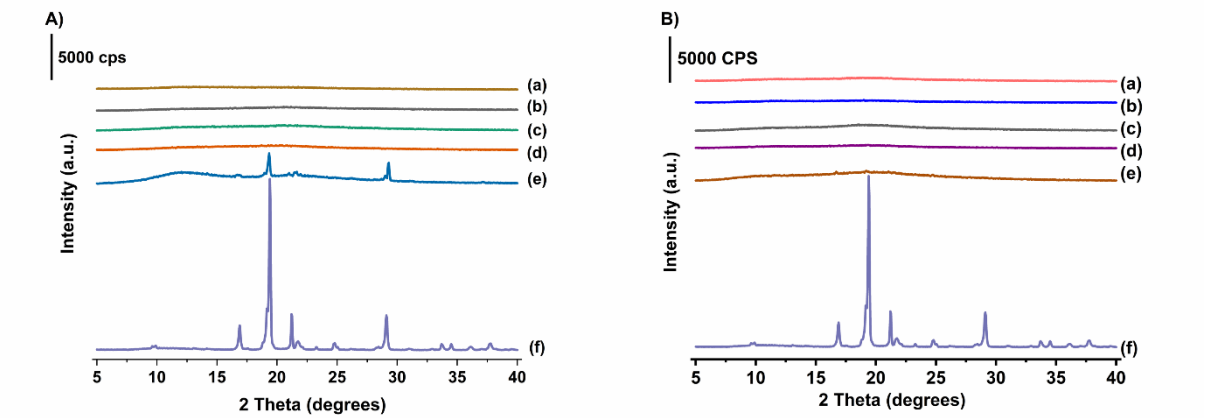

Figure 2. PXRD of HCTZ formulations: A) PVP/VA with (a) SD 30% API (b) SD 40% API (c) CP 30% API (d) CP 40% API (e) Physical Mixture (PM) with PVP/VA and 5% (w/w) crystalline API loading and (f) crystalline HCTZ. B) Soluplus® with (a) SD 30% API (b) SD 40% API (c) CP 30% API (d) CP 40% API (e) Physical Mixture (PM) with Soluplus® and 5% (w/w) crystalline API loading and (f) crystalline HCTZ.

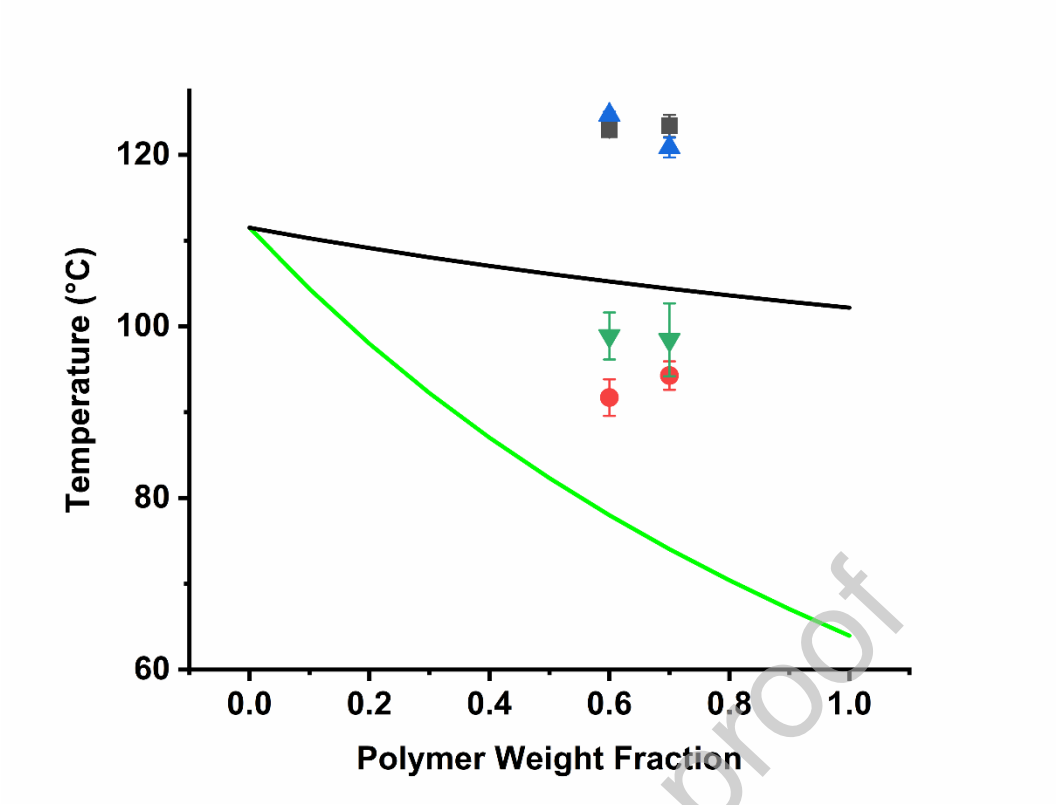

Figure 3. Glass transition temperature (T_g) predicted by the Gordon-Taylor equation. Solid line: black - HCTZ:PVP/VA predicted T_g, green - HCTZ:Soluplus predicted T_g. Experimentally obtained values: triangle - SD HCTZ with PVP/VA; square - CP HCTZ with PVP/VA; inverted triangle - SD HCTZ with Soluplus®; circle - CP HCTZ with Soluplus®.

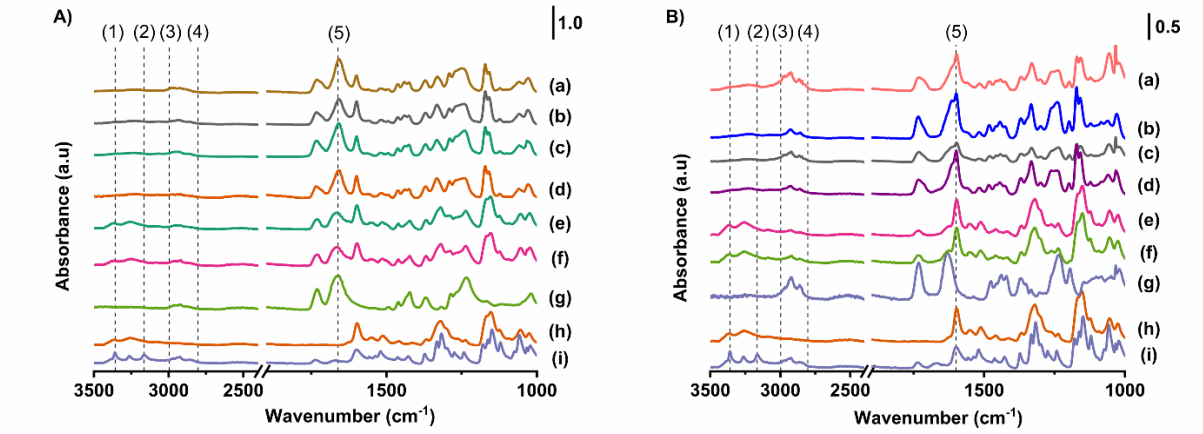

Figure 4. ATR FTIR of formulations with HCTZ: A) PVP/VA with (a) SD 30% API (b) SD 40% API (c) CP 30% API (d) CP 40% API (e) Physical Mixture (PM) with PVP/VA and 30% (w/w) amorphous API loading, (f) Physical Mixture (PM) with PVP/VA and 40% (w/w) amorphous API loading (g) PVP/VA (h) melt-quenched HCTZ (i) crystalline HCTZ. B) Soluplus® with (a) SD 30% API (b) SD 40% API (c) CP 30% API (d) CP 40% API (e) Physical Mixture (PM) with Soluplus® and 30% (w/w) amorphous API loading and (f) Physical Mixture (PM) with Soluplus® and 40% (w/w) amorphous API loading (g) Soluplus® (h) melt-quenched HCTZ (i) crystalline HCTZ. Reference Lines A) (1), (2), (3), (4), and (5) correspond to wave numbers of 3359, 3165, 2997, 2804, and 1661, respectively and B) (1), (2), (3), (4), and (5) correspond to wave numbers of 3359, 3165, 2997, 2804, and 1600, respectively.

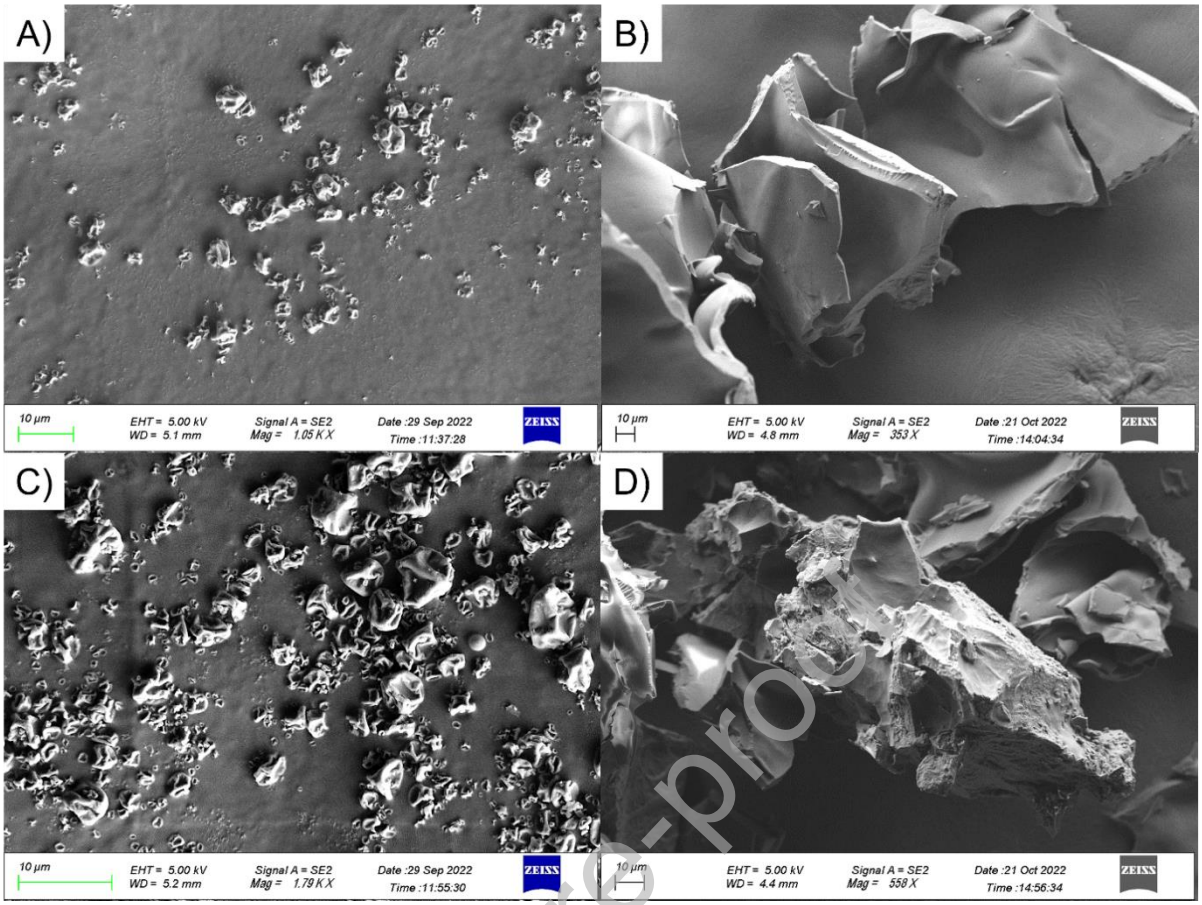

Figure 5. SEM images of formulations with HCTZ: A) Spray dried PVP/VA with 40% API, B) Co-precipitated PVP/VA with 40% API, C) Spray dried Soluplus® with 40% API , D) Co-precipitated Soluplus® with 40% API.

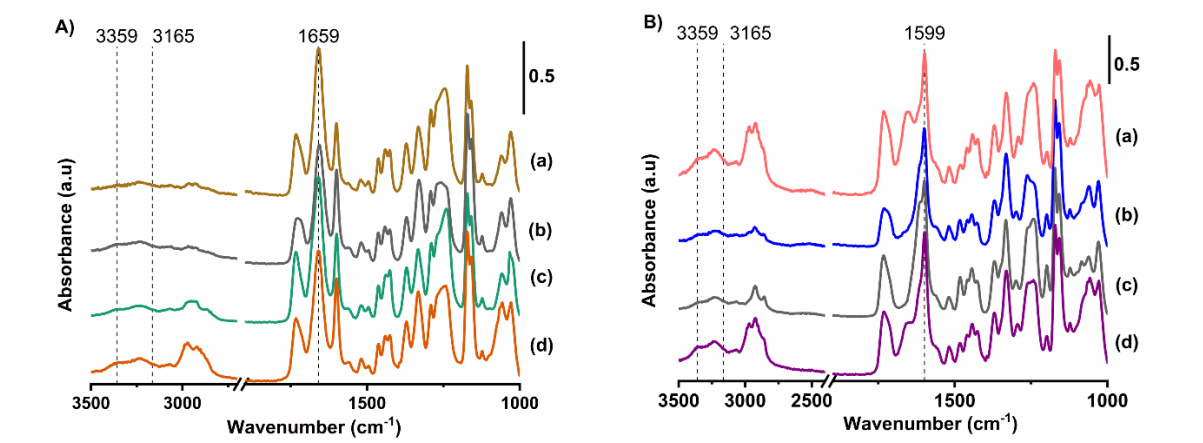

Figure 6. ATR FTIR of formulations with HCTZ of samples kept at 25 ^{o}C/75% RH for 4 weeks: A) PVP/VA with (a) SD 30% API (b) SD 40% API (c) CP 30% API (d) CP 40% API. B) Soluplus® with (a) SD 30% API (b) SD 40% API (c) CP 30% API (d) CP 40% API.

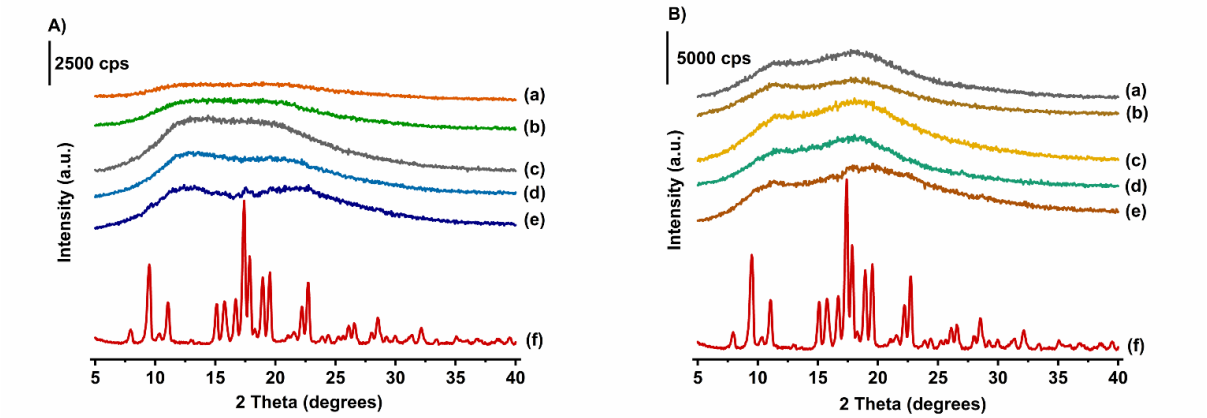

Figure 7. PXRD of SIM formulations: A) PVP/VA with (a) SD 30% API (b) SD 40% API (c) CP 30% API (d) CP 40% API (e) Physical Mixture (PM) with PVP/VA 64 and 5% (w/w) crystalline API loading and (f) crystalline SIM. B) Soluplus with (a) SD 30% API (b) SD 40% API (c) CP 30% API (d) CP 40% API (e) Physical Mixture (PM) with Soluplus and 5% (w/w) crystalline API loading and (f) crystalline SIM.

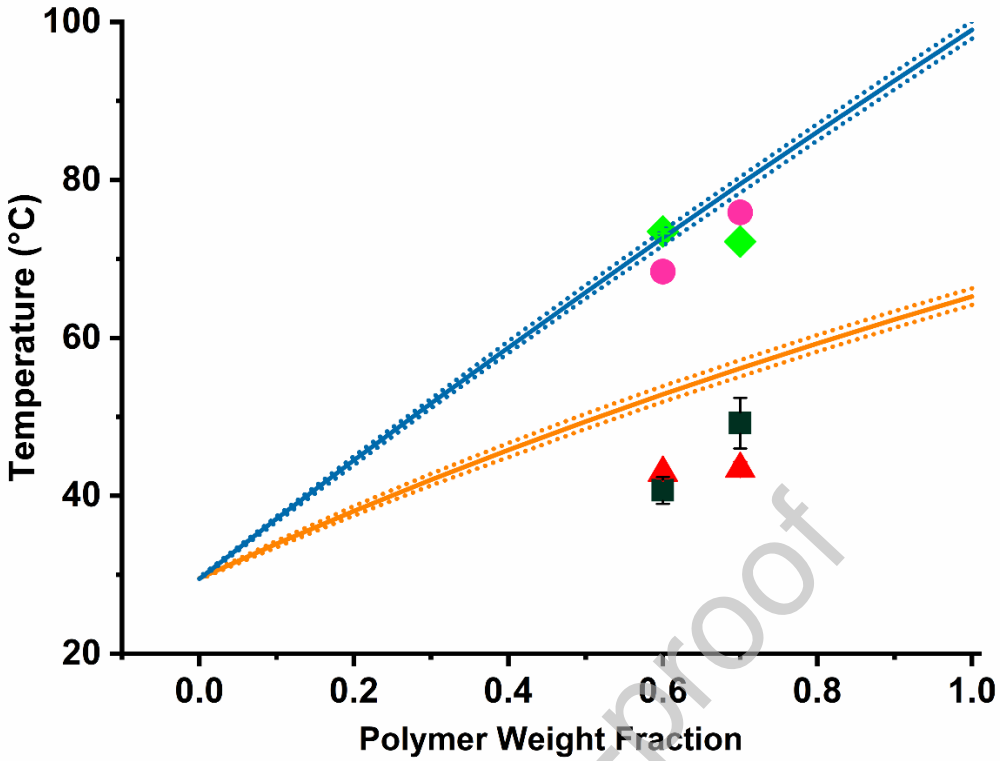

Figure 8. Glass transition temperature (T_g) values predicted by Gordon-Taylor equation. Solid line: blue - SIM:PVP/VA predicted T_g, orange - SIM:Soluplus® predicted T_g. The dotted curves are the error margins for the model. Experimentally obtained values: circle - SD SIM with PVP/VA; rhombus - CP SIM with PVP/VA; square - SD SIM with Soluplus®; triangle CP SIM with Soluplus®.

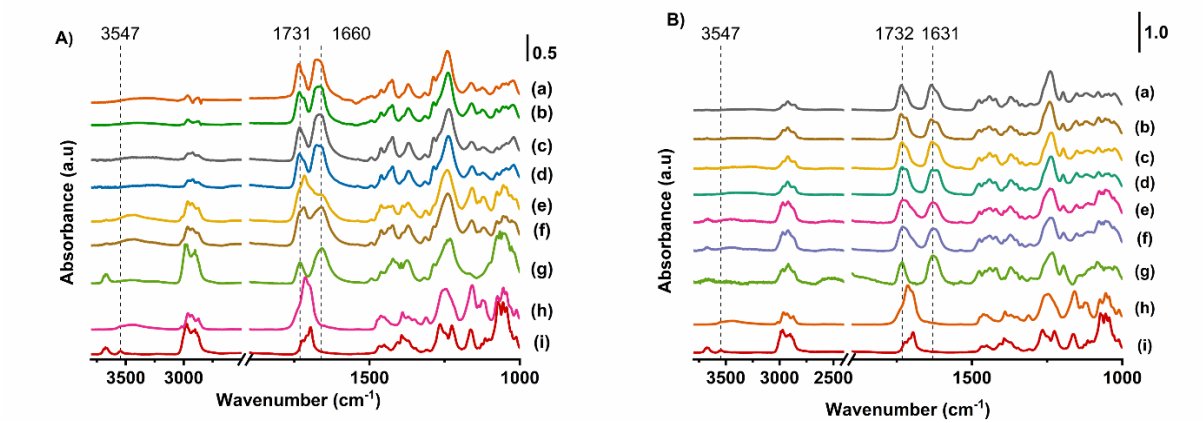

Figure 9. ATR FTIR of formulations with SIM: A) PVP/VA with (a) SD 30% API (b) SD 40% API (c) CP 30% API (d) CP 40% API (e) Physical Mixture (PM) with PVP/VA and 30% (w/w) amorphous API loading, (f) Physical Mixture (PM) with PVP/VA and 40% (w/w) amorphous API loading (g) PVP/VA (h) melt-quenched SIM (i) crystalline SIM. B) Soluplus® with (a) SD 30% API (b) SD 40% API (c) CP 30% API (d) CP 40% API (e) Physical Mixture (PM) with Soluplus® and 30% (w/w) amorphous API loading and (f) Physical Mixture (PM) with Soluplus® and 40% (w/w) amorphous API loading (g) Soluplus® (h) melt-quenched SIM (i) crystalline SIM.

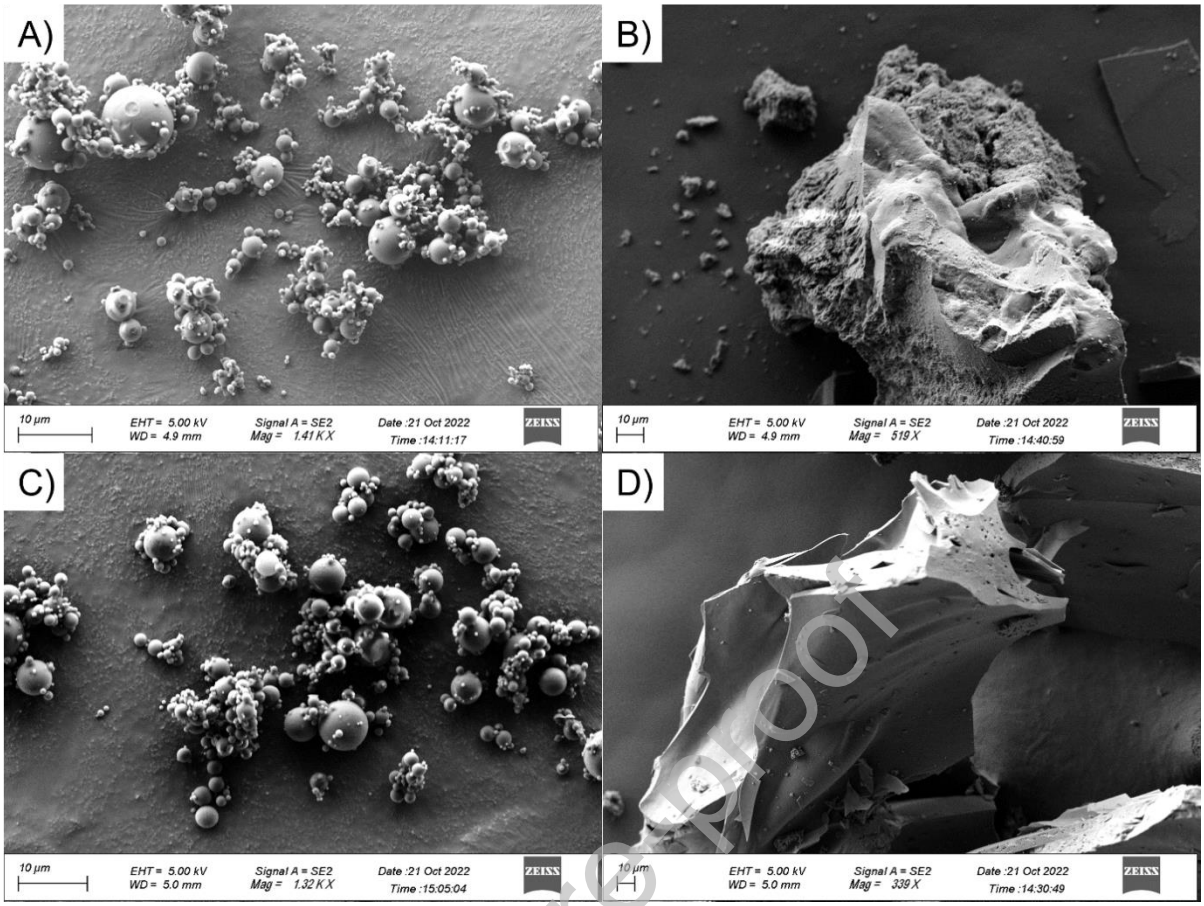

Figure 10. SEM images of formulations with SIM: A) Spray dried PVP/VA with 40% API, B) Co-precipitated PVP/VA with 40% API, C) Spray dried Soluplus® with 40% API, D) Co-precipitated Soluplus® with 40% API.

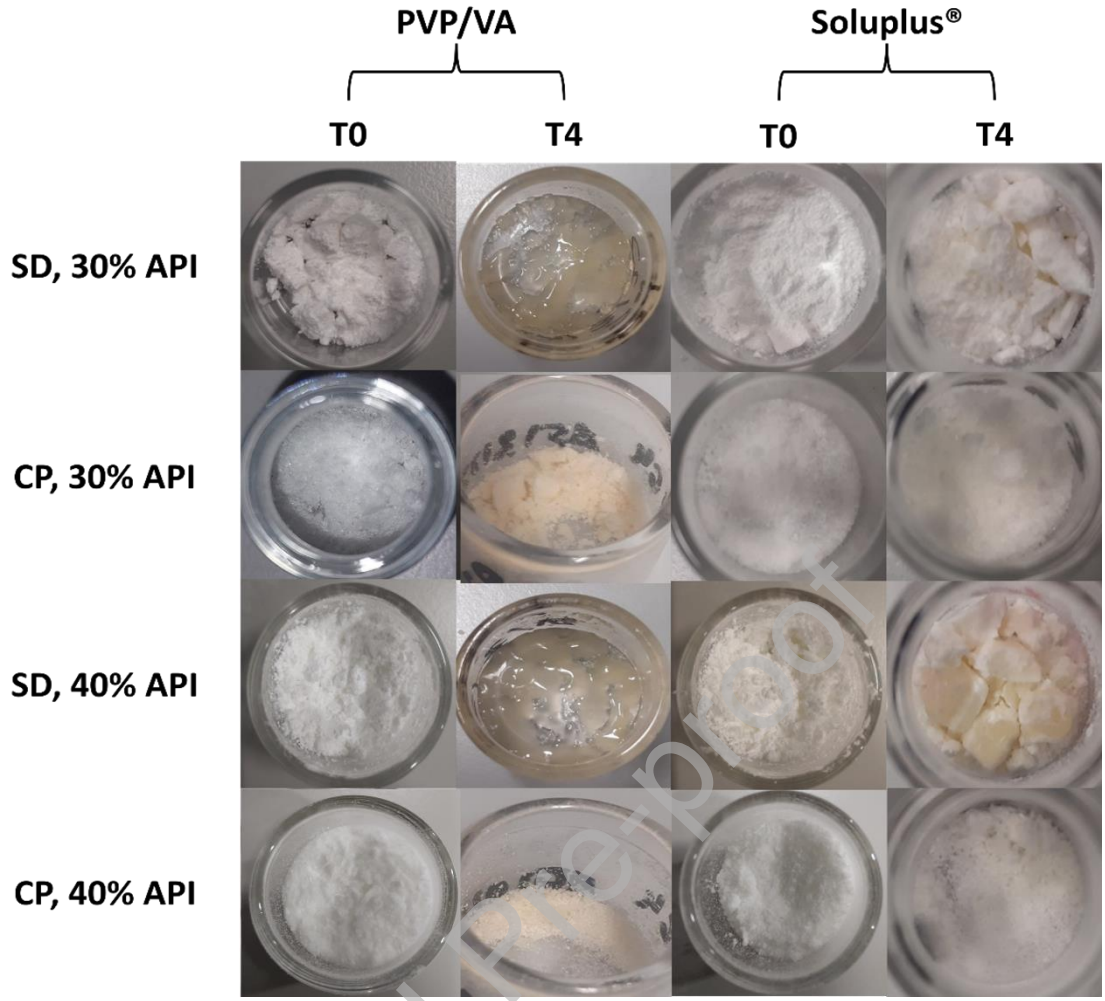

Figure 11. Photographs of SIM - SD and SIM - CP systems at T0 and T4.

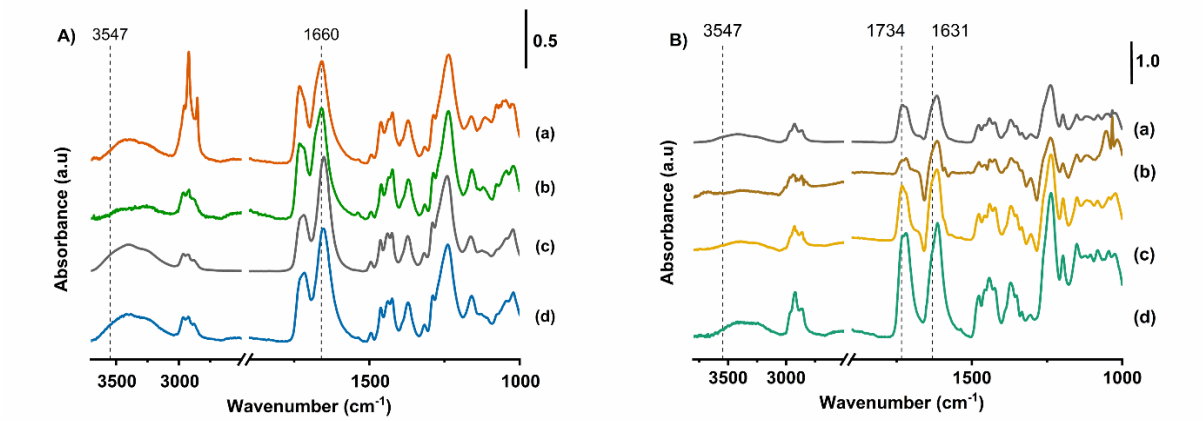

Figure 12. ATR FTIR of formulations with SIM of samples kept at 25 ^{o}C/75% RH for 4 weeks: A) PVP/VA with (a) SD 30% API (b) SD 40% API (c) CP 30% API (d) CP 40% API. B) Soluplus® with (a) SD 30% API (b) SD 40% API (c) CP 30% API (d) CP 40% API.

Table 1. Physicochemical properties of Hydrochlorothiazide (HCTZ) and Simvastatin (SIM).

Property	**HCTZ**	**SIM**
Molecular weight	297.7[48]	418.3[49]
Hydrogen bond acceptors	7[48]	5[49]
Hydrogen bond donors	3[48]	1[49]
Melting temperature (°C)	271*	140*
T_g (°C)	116*	32*
Aqueous solubility (mg/mL)	0.7[50]	0.03[51]

* data obtained experimentally (described in materials and methods section)

Table 2. The solubility of HCTZ, polymer (Soluplus®) and the model co-precipitated HCTZ:Soluplus® (30:70) system in different solvent to antisolvent ratio mixes and at different temperatures.

Temperature (°C)	Solvent: Antisolvent ratio	Solubility of HCTZ (mg/mL) in solvent mix	Solubility of polymer (mg/g) in solvent mix	Solubility of co-precipitated amorphous system (mg/g) in solvent mix
5	1:4	0.03	4.69	0.59
10	1:4	0.04	4.91	0.63
15	1:4	0.05	6.12	0.92
10	1:3	0.10	8.27	2.24

Table 3. Formulation compositions, obtained yields and solvent demand for HCTZ spray dried (SD) and co-precipitated (CP) systems.

Sample Composition	API Content (%w/w)		Polymer Content (%w/w)		Yield (%)		Solvent Demand ($mL/g_{product}$)	
	SD	CP	SD	CP	SD	CP	SD	CP
PVP/VA, 30% API	30.1 ± 1.9	28.8 ± 0.8	66.2 ± 1.9	68.2 ± 0.8	71.0 ± 2.0	65.1 ± 8.3	55.9	153.6
PVP/VA, 40% API	40.2 ± 1.1	38.9 ± 2.2	55.8 ± 1.1	58.2 ± 2.2	72.6 ± 2.5	66.2 ± 6.2	52.4	152.5
Soluplus®, 30% API	27.8 ± 2.1	26.6 ± 2.4	69.2 ± 2.1	70.2 ± 2.4	65.3 ± 3.3	57.0 ± 6.8	60.7	175.4
Soluplus®, 40% API	35.2 ± 1.0	35.7 ± 0.7	60.1 ± 1.0	60.5 ± 0.7	67.6 ± 3.5	62.5 ± 7.8	56.8	161.3

Table 4. The midpoint glass transition temperatures (T_gs) and residual moisture content of the HCTZ-based spray- dried and co-precipitated systems.

Sample Composition	T_g (°C)		Residual Moisture Content (%)	
	Spray Dried	Co-Precipitated	Spray Dried	Co-Precipitated
PVP/VA, 30% API	129.17 ± 0.28	133.21 ± 0.51	2.90 ± 0.26	3.05 ± 0.65
PVP/VA, 40% API	131.21 ± 0.37	132.89 ± 0.84	2.70 ± 0.82	2.88 ± 0.26
Soluplus®, 30% API	107.41 ± 1.88	101.68 ± 1.48	3.04 ± 0.11	2.94 ± 0.09
Soluplus®, 40% API	109.23 ± 0.76	101.48 ± 0.66	3.45 ± 0.27	3.30 ± 0.17

Table 5. Particle size d_{10}, d_{50} and d_{90} of spray-dried and co-precipitated HCTZ products.

Sample Composition	Spray Dried Product			Co-precipitated Product		
	D_{10} (μm)	**D_{50} (μm)**	**D_{90} (μm)**	**D_{10} (μm)**	**D_{50} (μm)**	**D_{90} (μm)**
PVP/VA, 30% API	1.0 ± 0.1	2.2 ± 0.2	4.3 ± 0.1	76.1 ± 3.5	321.2 ± 29.7	778.8 ± 68.2
PVP/VA, 40% API	1.0 ± 0.1	2.1 ± 0.1	4.5 ± 0.4	32.2 ± 10.2	259.2 ± 20.8	989.4 ± 107.3
Soluplus®, 30% API	1.0 ± 0.1	2.5 ± 0.2	5.2 ± 0.1	33.1 ± 4.8	155.8 ± 29.1	243.3 ± 41.2
Soluplus®, 40% API	1.2 ± 0.1	2.7 ± 0.1	5.7 ± 0.1	9.2 ± 1.1	179.7 ± 59.9	1134.4 ± 351.9

Table 6. Bulk and tapped density and Carr's Compressibility Index (CCI) for spray-dried and co-precipitated HCTZ systems.

Sample Composition	Bulk density (g/cm^3)		Tapped density (g/cm^3)		Carr's Compressibility Index	
	Spray Dried	Co-Precipitated	Spray Dried	Co-Precipitated	Spray Dried	Co-Precipitated
PVP/VA, 30% API	0.29 ± 0.01	0.28 ± 0.04	0.47 ± 0.01	0.44 ± 0.05	37.78 ± 2.43	36.36 ± 3.29
PVP/VA, 40% API	0.29 ± 0.05	0.29 ± 0.08	0.49 ± 0.09	0.48 ± 0.07	42.01 ± 4.43	34.68 ± 3.17
Soluplus®, 30% API	0.27 ± 0.02	0.31 ± 0.01	0.41 ± 0.02	0.41 ± 0.02	34.61 ± 3.23	26.97 ± 2.53
Soluplus®, 40% API	0.23 ± 0.02	0.32 ± 0.02	0.36 ± 0.03	0.42 ± 0.04	35.86 ± 3.48	23.80 ± 2.31

Table 7. The midpoint glass transition temperatures (T_gs) and residual moisture content of the HCTZ-based spray- dried and co-precipitated systems kept at 25°C/ 75% RH for four weeks (T4).

Sample Composition	T_g (°C)		Residual Moisture Content (%)	
	Spray Dried	Co-Precipitated	Spray Dried	Co-Precipitated
PVP/VA, 30% API	129.42 ± 0.68	132.34 ± 0.72	5.25 ± 0.46	5.85 ± 2.17
PVP/VA, 40% API	132.22 ± 0.26	133.33 ± 0.76	4.92 ± 0.16	3.87 ± 1.37
Soluplus®, 30% API	111.22 ± 4.07	109.27 ± 8.33	3.07 ± 0.21	4.38 ± 0.33
Soluplus®, 40% API	112.86 ± 2.27	105.54 ± 1.14	2.78 ± 0.10	4.68 ± 0.12

Table 8. The equilibrium solubility of physical mixture of SIM and Soluplus® at 25 °C and the solubility of the co-precipitated SIM and Soluplus® system in a ratio 30:70 at -10 °C.

Temperature (°C)	**Solvent: Antisolvent ratio**	**Solubility of co – precipitated amorphous system (mg/g solvent mix)**	**Solubility of SIM (mg/mL)**
25	1:30	N/A	0.20 ± 0.05
-10	1:30	1.5 ± 0.3	0.03 ± 0.01

Table 9. Formulation compositions, obtained yields and solvent demand for SIM spray dried (SD) and co-precipitated (CP) systems.

Sample Composition	API Content (%w/w)		Polymer Content (%w/w)		Yield (%)		Solvent Demand ($mL/g_{product}$)	
	SD	CP	SD	CP	SD	CP	SD	CP
PVP/VA, 30% API	30.1 ± 0.5	28.5 ± 1.1	67.1 ± 0.5	66.5 ± 1.1	76.1 ± 3.0	53.9 ± 8.0	25.6	162.1
PVP/VA, 40% API	38.7 ± 1.1	38.2 ± 1.2	58.9 ± 1.1	59.1 ± 1.2	81.0 ± 4.5	57.5 ± 7.5	24.8	153.1
Soluplus®, 30% API	31.1 ± 1.8	30.3 ± 1.7	68.9 ± 1.8	67.1 ± 1.7	79.4 ± 3.1	59.1 ± 5.1	25.1	148.9
Soluplus®, 40% API	38.6 ± 0.9	39.7 ± 1.0	61.7 ± 0.9	63.3 ± 0.2	82.6 ± 3.6	66.1 ± 4.2	24.2	133.1

Table 10. The midpoint glass transition temperatures (T_gs) and residual moisture content of the SIM-based spray- dried and co-precipitated systems.

Sample Composition	T_g (°C)		Residual Moisture Content (%)	
	Spray Dried	Co-Precipitated	Spray Dried	Co-Precipitated
PVP/VA, 30% API	80.93 ± 0.83	80.17 ± 1.09	2.65 ± 0.07	2.06 ± 0.08
PVP/VA, 40% API	74.53 ± 0.34	79.38 ± 0.08	1.95 ± 0.49	1.85 ± 0.07
Soluplus®, 30% API	56.56 ± 1.47	58.40 ± 2.28	1.35 ± 0.21	1.40 ± 0.28
Soluplus®, 40% API	52.38 ± 1.23	54.18 ± 1.40	1.20 ± 0.14	1.20 ± 0.14

Table 11. Particle size, d_{10}, d_{50} and d_{90} of spray-dried and co-precipitated SIM products.

Sample Composition	Spray Dried Product			Co-precipitated Product		
	D_{10} (μm)	**D_{50} (μm)**	**D_{90} (μm)**	**D_{10} (μm)**	**D_{50} (μm)**	**D_{90} (μm)**
PVP/VA, 30% API	1.5 ± 0.1	5.9 ± 0.1	15.6 ± 0.8	38.6 ± 3.2	256.1 ± 52.2	858.4 ± 110.9
PVP/VA, 40% API	1.2 ± 0.1	4.5 ± 0.7	20.3 ± 10.6	24.2 ± 2.1	176.5 ± 40.9	753.7 ± 197.6
Soluplus®, 30% API	1.4 ± 0.2	5.9 ± 1.6	310.7 ± 50.4	33.9 ± 3.5	155.8 ± 29.1	721.7 ± 149.7
Soluplus®, 40% API	1.4 ± 0.1	5.3 ± 0.2	424.9 ± 91.9	35.1 ± 4.2	174.7 ± 29.4	561.5 ± 121.3

Table 12. Bulk and tapped density and Carr's Compressibility Index (CCI) for spray-dried and co-precipitated SIM systems.

Sample Composition	Bulk density (g/cm^3)		Tapped density (g/cm^3)		Carr's Compressibility Index	
	Spray Dried	Co-Precipitated	Spray Dried	Co-Precipitated	Spray Dried	Co-Precipitated
PVP/VA, 30% API	0.33 ± 0.04	0.26 ± 0.03	0.47 ± 0.06	0.32 ± 0.04	28.86 ± 3.35	19.84 ± 3.29
PVP/VA, 40% API	0.37 ± 0.04	0.25 ± 0.02	0.48 ± 0.04	0.29 ± 0.01	23.87 ± 5.09	16.63 ± 4.70
Soluplus®, 30% API	0.26 ± 0.04	0.19 ± 0.04	0.39 ± 0.07	0.24 ± 0.05	32.66 ± 5.27	20.97 ± 1.53
Soluplus®, 40% API	0.29 ± 0.01	0.22 ± 0.06	0.39 ± 0.07	0.27 ± 0.06	27.19 ± 6.28	18.96 ± 3.77

Table 13. The midpoint glass transition temperature (T_g) and residual moisture content of the SIM-based spray- dried and co-precipitated systems kept at 25°C/ 75% RH for four weeks (T4).

Sample Composition	T_g (°C)		Residual Moisture Content (%)	
	Spray Dried	Co-Precipitated	Spray Dried	Co-Precipitated
PVP/VA, 30% API	57.09 ± 2.35	60.14 ± 3.27	4.50 ± 0.14	4.05 ± 0.78
PVP/VA, 40% API	56.18 ± 0.92	58.05 ± 0.55	4.20 ± 0.71	3.95 ± 0.49
Soluplus®, 30% API	49.39 ± 0.17	52.75 ± 0.24	3.45 ± 0.10	2.65 ± 0.07
Soluplus®, 40% API	53.29 ± 0.74	54.86 ± 1.53	2.85 ± 0.35	3.10 ± 0.14